École polytechnique de Louvain

Estimating the environmental impact of deep-sea mining

Construction of a consistent hydrodynamic model

Author: **Igor de Streel**
Supervisors: **Eric Deleersnijder, Emmanuel Hanert**
Readers: **Vincent Legat, Valentin Vallaeys, Céline Taymans**
Academic year 2019–2020
Master [120] in Mechanical Engineering

Abstract

New technologies and the green transition are pushing our consumption further than ever. Mining is thus essential to follow the trend. But mines are depleting themselves. Hopefully there is a possibility for an almost limitless supply of some metals. The Clarion Clipperton fracture zone is full of polymetalic nodules. These stones barely bigger than a fist abound in ores. They contain cobalt, nickel, copper and manganese and could help us achieve the green transition.
The only obstacle is that these nodules are lying on the seabed at more than 4000m underwater. Collecting them is thus a real challenge but the environmental impact of the collection could also be really harmful for the local fauna and flora. It is thus essential to evaluate the environmental impact of deep sea mining. The biggest impact will come from plumes of sediment released during the collection of the nodules. Tracing those plumes is the key towards the evaluation of the environmental impact.
This thesis will develop the method to build a model using the 3D version of the Second-generation Louvain-la-Neuve Ice-Ocean Model. That model will then be developed in the Clarion Clippertone zone in order to simulate the currents to later trace the plumes.

Acknowledgement

First of all I would like to thank Professor Emmanuel Hanert for his supervision, his guidance and his support during the writing of this thesis.

Then I would like to thank Valentin Vallaeys, Thomas Dobberlaere adn François Duquesne for their help with SLIM and their for their avalaibility.

I am also gratefull to Professor Eric Deleersnijder who is SLIM founding father and to Celine Taymans without whom this thesis would not have been possible

Finally I would like to thank John Moraine for his proof-reading.

Contents

Chapter 1

Introduction

1.1 Context

Since prehistoric time, mining is a part of human's activities. Prehistoric men started to mine to procure themselves flint and other rocks in order to build some tools. Since then mining has evolve and the desired material too. The human is not looking anymore for flint in galleries near the surface, he is now searching for cobalt at more than 4000m deep into the ocean! The human being is always looking further and deeper for new mines in order to fulfil our modern way of life, our massive consumption.
Indeed, as it has been said: "if you can't grow it you have to mine it" you can quickly remark that a lot of the materials that surround us have thus to be mined. And our rising demand in mining is pushed by economic and demographic growth. Unfortunately the reserves are not unlimited, they are depleting. There is thus a need to find new ones. One possibility is to collect the ores directly on the ocean floor and in particular in the CCZ (Clarion Clipperton zone fig: 1.1).

Figure 1.1: Clarion Clippertone Fracture Zone

This area is of a great interest as it is rich in polymetalic nodules, a valuable material. It is precisely these nodules that Global Sea Mineral Resources (GSR), a subsidiary of dredging firm DEME (Dredging, Environmental and Marine Engineering), is interested in collecting in order to exploit. GSR is using its experience in dredging to adapt and to diversify itself in order to be able to collect those nodules

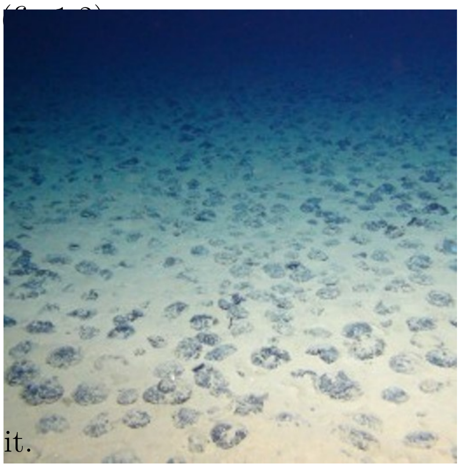

Figure 1.2: Polymetalic nodules found in the CCZ.

For deep-sea mining to be launched at industrial scale, it is important to be at the same time economically viable, politically acceptable and environmentally safe. There are thus some critical factors that will push towards deep-sea mining. On the contrary there also exist some counter arguments to such a practice, these need to be evaluated subsequently in order to decide wether deep-sea mining is really worth it.

1.1.1 Economic aspects

When considering the economic aspect of deep-sea mining it might at first seem kind of odd to mine at such great depths. Indeed, how interesting can it really be to go at more than 4000 meters underwater in the ocean to get some nodules. Is there really space for a return on investment?
There might be. Rarefaction of critical materials and rare metals are pushing towards new reserves and thus new areas to explore. Kris Van Nijen, general manager at GSR says: "After all, research shows that the quality of the ores on the land is declining: an ore from a mine used to contain on average four per cent copper ; now that is less than one per cent. As a result, it requires more and more energy to extract less and less raw material."[1]

In addition to providing copper, polymetalic nodules also contain three others researched minerals. They consist thus out of 4 different metals that are all valuable. They contain manganese at a concentration of 27 to 30%, cobalt at a concentration of 0.2 to 0.25%, nickel at a concentration of 1.25 to 1.5% and copper at a concentration of 1 to 1.4% [13]. All those concentrations are the equivalent of economical exploitable resources[1]. The concentration of each mineral is thus equivalent or higher than the concentrations found in the reserves [2]

[1]Resources are the inventory of everything geologists have been able to identify and quantify

[2]Reserves, form an exploitable subset of resources which corresponds to criteria of profitability, of feasibility (technical), economic, social (local population agreement) and environmental (permits)

of that mineral. But for deep-sea mining, the conditions of extraction are different. It is more difficult to reach the nodules because they lie on the seabed at more than 4000m depth. However when you reach them you just have to collect them from the seabed. There is thus no need for extraction quarries or tunnels. Also, because the nodules contains 4 different metals it gives the reserve a greater value not only because you have more ores to exploit but also because of the diversity of those ores. Indeed the nodules consisting out of different ores makes the extraction more stable economically. The total income per nodule will depend on 4 metals making it less sensitive to the market fluctuation of one of them.

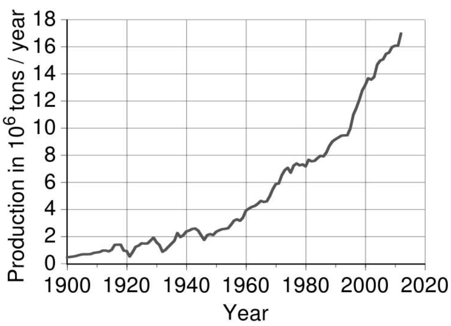

Figure 1.3: Copper production evolution and estimation. [2]

Among the exploitable metals, cobalt is really important because it is part of the critical raw materials matrix developed by the European Union. That matrix plots different metals depending on their future importance to the EU economy and on the risk associated with their supply (fig: 1.5).
All the metals found in the polymetalic nodules will be really important materials for the economy of the EU and that among those, cobalt will also have a supply risk (see fig:1.4).
The economic importance of those materials is linked to our rising need of materials. Recycling is not enough, the extraction needed is rising and recycling will not provide enough(see fig:1.3). Extraction remains vital to provide for these materials. For example, cobalt is a key material in all the technologies linked to the green transition. It will be used mostly in batteries for electrical vehicle but also for wind turbines and others new technologies [3].

New extraction sites of these materials can be a solution to the rising demand of the future. Especially knowing that the supply in the deep-sea is almost limitless. Indeed, the amount of nickel and cobalt between Hawaii and Mexico (in the CCZ) is estimated to be respectively 6 and 3 times the earth's reserve [13].
The rising demand, the richness of the ores and the almost limitless supply are all economic factors that are pushing towards deep-sea mining. On the other hand the difficulty to reach the nodules at more than 4000m is the real economic challenge that may limit the feasibility of deep-sea mining.

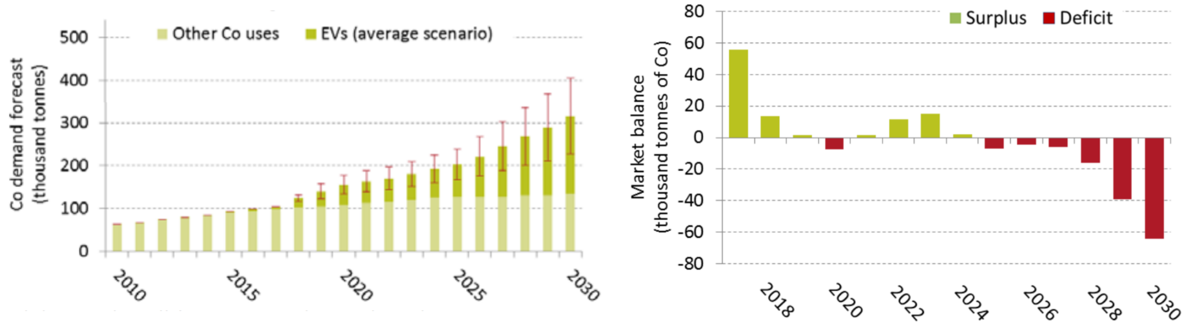

(a) Cobalt demand: evolution and prevision

(b) Cobalt market balance prevision

Figure 1.4: Cobalt supply risk

1.1.2 Political aspects

The politic stakes around deep-sea mining are varied. To start, there is for cobalt a supply risk in the future. That risk is linked to the origins of cobalt. Indeed, for the moment most of the cobalt comes from Democratic Republic of Congo (DRC) and China. But DRC's political instability is a constant threat to the supply. Also, from an ethical point of view, there is no control on the extraction. The extraction could thus be tainted with children labour.[6]
That leaves us with a supply from China. But China's supply is also at risk. Indeed a monopoly is always risky and the fact that China has already limited its exportation in the past[3] reinforces the instability of supply.

[3]In 2010, China's export quotas of rare earth was reduced by 40%.[7]

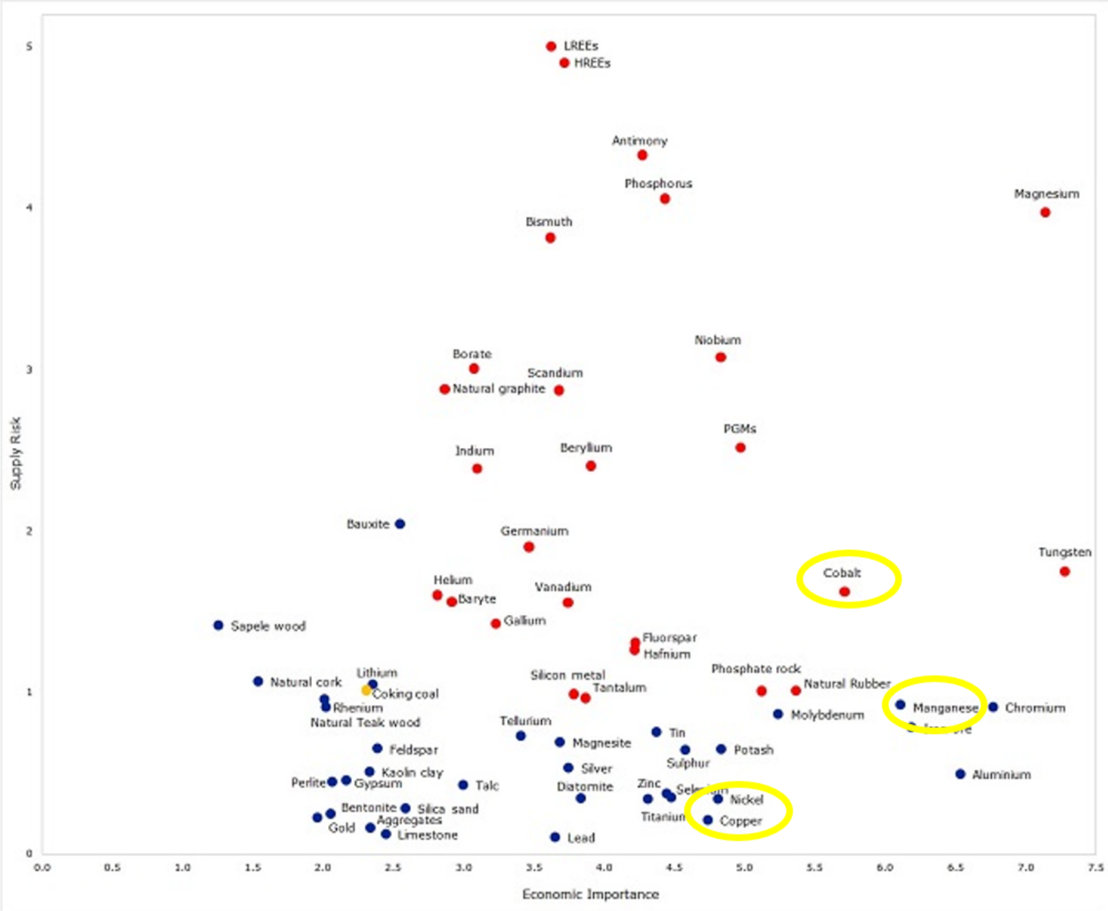

Figure 1.5: The critical raw material matrix defined by the EU, the abscissa shows the economic importance of the material and the ordinate shows the supply risk. Based on those two criteria, the EU can make a list of the critical raw materials.[8]

Adding a new source to the supply could get us free of the dependency towards one or another political issue. It would make the supply stronger.

In addition to the supply risk, dividing the exploitation sites between the different contractors is also a big challenge. That is the job of the ISA (International Seabed Authority). The exploitation zones being in international waters they are common to everyone on earth, it is thus important to be fair in the division and to avoid a rush that will end in "first arrived first served". The ISA is thus regulating the exploitation of the deep-sea in order to limit and to monitor its exploitation. They also decide which zone will be protected (Area of Particular Environment Interest, see fig:1.6) in order to protect deep-sea fauna and flora.

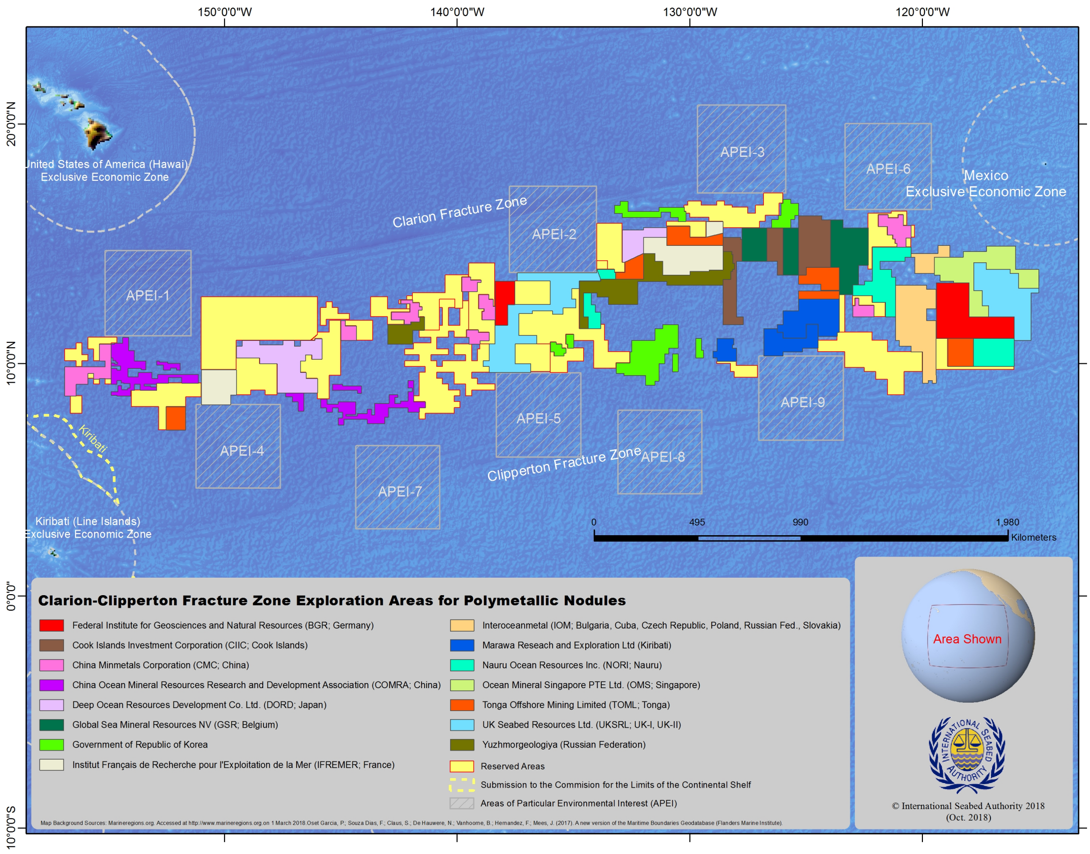

Figure 1.6: ISA repartition of the CCZ, it shows the different contract of exploitation and the protected zones, the APEI (Area of Particular Environment Interest).[9]

1.1.3 Ecological aspects

Another important factor that we need to take into account when considering deep-sea mining is its ecological impact. Indeed, even if we do not know a lot about the fauna and the flora in the deep ocean, we do know that there is a great diversity in the benthic fauna and flora and that we need to protect it. The ISA manages the activities in the ocean and the protection of the ocean: "As part of ISA's responsibilities is to take the necessary measures with respect to activities in the Area to ensure the effective protection of the marine environment from harmful effects which may arise from activities in the Area."[10]. They want to take things slowly and avoid an intensive exploitation where we measure the ecological impact afterwards. It is thus really important for each contractor to study and calibrate the possible impact of their exploitation. The damages can be caused by the removal of habitats and materials, by the plumes, by the lights, by the noises and the vibrations or by other disturbances (fig:1.7).

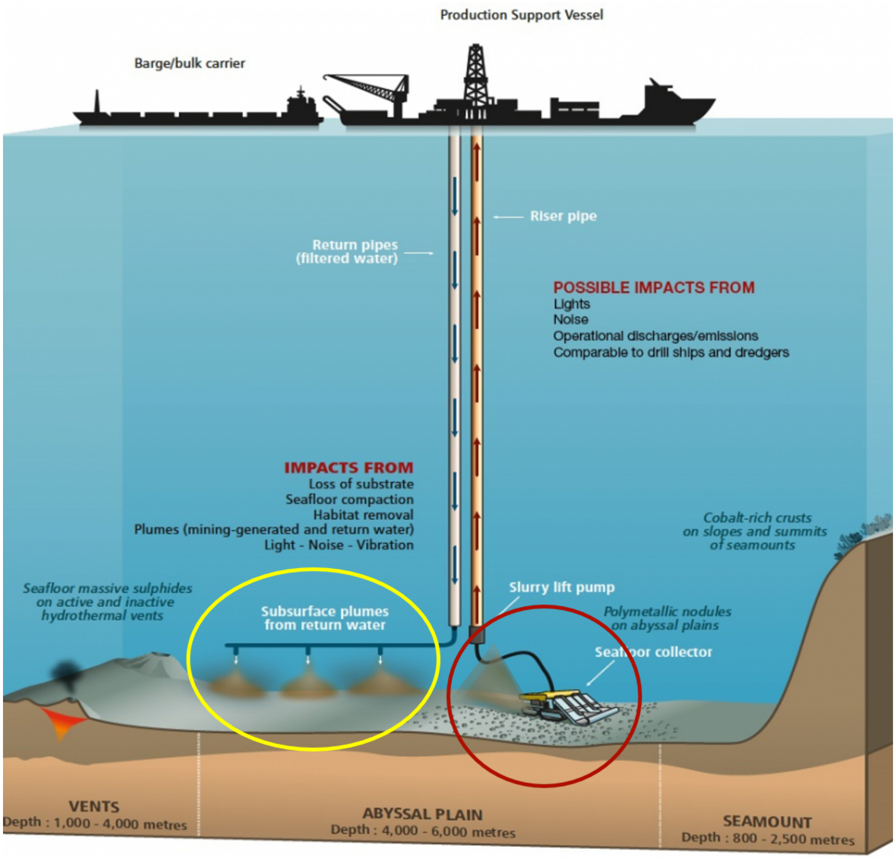

Figure 1.7: deep-sea mining plan and potential impacts. The red circles shows the plumes generated by the mining and the yellow circle shows the return plumes.[12]

All these disturbances will have an impact on the ocean ecosystem. According to Thomas Peacock, the impact will be devastating in the direct mining area; "In the direct mining area [...] the impact is going to be very high and I don't think there's any reasonable expectation that any life that exists in that area will survive. That will be lost and there's evidence of that." [13]

But the impact of deep-sea mining is to be put in perspective with the ecological impact of land mines. Both have or will have an ecological impact. The goal is here to minimize it and to see if deep-sea mines could help decrease the total ecological impact of mines.

The biggest concern about the ecological impact is linked to the deposition of plumes generated during the mining. The plumes are generated in two ways. The first group of plumes are generated directly when picking up the nodules. The collector vehicle picks up 10 to 45cm of the top of the seabed, generating the

plumes directly just above the seabed. Those plumes represent 95% of the plumes generated. When picking up the nodules, the collector vehicle picks up also a part of the seabed and all of it is send to the boat. There, the separation is done and the unwanted sediments are sent back in the ocean. That's where the last 5% of the plumes are from. Those last 5% will be released under the pycnocline but the precise depth is not defined yet (see fig: 1.7).
Those plumes will then be carried away by the currents and they will recover a part of the seabed having there an impact on the local fauna and flora. The ecologic impact of the plumes will thus be proportional to dispersion of those.
To evaluate the impact of the plumes we need to be able to track them. This can be done thanks to data collection and model simulations. But data only gives an idea of the water and the sediments dynamics at a particular location in space and during a particular period of time.
A simulation can be adapted and would help us track the plumes on several places and at any time needed (provided that you have got the forcing data). It would thus help estimate the ecological impact and adapt the mining condition in order to minimise the impact of the plumes.
The goal of this thesis is thus to develop a realist hydrodynamic simulation. That simulation can afterwards be used in order to track the plumes and to estimate the environmental impact of deep-sea mining.

1.1.4 Scope of the simulation

The simulation will be focused on the exploitation domain of GSR inside the CCZ zone (see fig:1.6). We will focus on the zone B4, the environmental baseline is there complete and suitable for future mining projects [**?**] and a lot of studies led by the GSR were done inside that zone. That will give us in-situ data to compare against. Also, we will focus our study on the seabed because it is there that the sediment plumes will be created or released and tracked.
The simulations will take place in 2017 and the month will depend on which mooring we compare it to. But generally we will compare our results to the 4^{th} mooring because of its precision near the bottom of the ocean and the longevity of the collected date. The simulation will thus take place in September.

Chapter 2

Mathematical Model

2.1 Three dimensionnal oceanic model

In order to compute a 3D oceanic model, it is important to understand the physical principles that rule the hydrodynamic of the ocean and their equations. They are the three-dimensional hydrostatic equations. Those equations are based on the conservation laws and they are applied on a certain domain (see fig: 2.1).

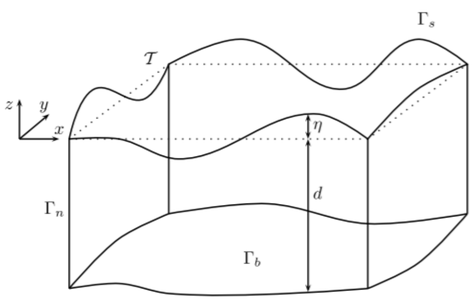

Figure 2.1: Ocean domain Ω where the 3D oceanic model can be computed and the different notations [?]

The domain where those equations are applied, Ω, is limited by different boundaries. Γ_b, is the bottom boundary, the seabed; it is time invariant. Γ_n are the lateral boundaries that can be either open or closed; their position (x,y) is also time independent. Finally Γ_s represents the surface boundary its position is time dependent. Indeed the boundary is fixed with d, the total bathymetry and η the surface elevation and the surface evolution changes with the time.

2.1.1 Three-dimensional hydrostatic equations

The three-dimensional hydrostatic equations are then used to calculate the temporal evolution of several variables inside our domain. The variables are the following:

- $\mathbf{u}(t, x, y, z)$, the horizontal velocity, it is composed of u(t,x,y,z) the zonal velocity and v(t,x,y,z) the meridional velocity.

- $w(t, x, y, z)$, the vertical velocity
- $p(t, x, y, z)$, the pressure
- $\eta(t, x, y)$, the surface elevation
- $S(t, x, y, z)$, the salinity
- $T(t, x, y, z)$, the temperature

The momentum equation

The momentum equation is based on the conservation law of the same name, its expression is the following:

$$\begin{aligned} \mathbf{P}(t) &= \int_{\Omega(t)} \rho \mathbf{v} dv \\ \frac{D}{Dt}\mathbf{P}(t) &= \mathbf{F}^c + \mathbf{F}^d \end{aligned} \tag{2.1}$$

It means that the changes of momentum of a domain ($\mathbf{P(t)}$) are provoked by the forces that act on that domain. Those forces can be contact forces ($\mathbf{F}^c$) or distance forces ($\mathbf{F}^d$). Developing the momentum equation (eq: 2.1) in our domain we then arrive at the following equation.

$$\begin{aligned} \frac{\partial \mathbf{u}}{\partial t} + \nabla_h \cdot (\mathbf{uu}) + \frac{\partial (w\mathbf{u})}{\partial z} &= \nabla_h \cdot (\nu_h(\nabla_h \mathbf{u} + (\nabla_h \mathbf{u})^T)) + \frac{\partial}{\partial z}(\nu \frac{\partial u}{\partial z}) \\ &- f e_z \wedge \mathbf{u} - \frac{1}{\rho_0} \nabla_h p \end{aligned} \tag{2.2}$$

Where $\nabla_h = e_x \frac{\partial}{\partial x} + e_y \frac{\partial}{\partial y}$ is the horizontal gradient operator, ρ_0 is the reference density, ν_h is the horizontal viscosity, ν is the vertical eddy viscosity, f is the Coriolis factor. Those four last are parameters determined determined by the model chosen.
The left term represents the material derivative of the momentum and the right term represents the different forces. The contact forces are the shear stresses linked to the velocity gradient (two first terms). The distance forces are exerted here by Coriolis and the gravity under the form of a pressure gradient (two last terms).

The continuity equation

The continuity equation is based on the mass conservation law, it is the following:

$$\begin{aligned} M(t) &= \int_{\Omega}(t) \rho dv \\ \frac{D}{Dt} M(t) &= 0 \end{aligned} \tag{2.3}$$

This law states that the variation of mass into the domain is equal to the flow going through the borders. It gives thanks to Boussinesq approximation the continuity equation (see eq: 2.4). The Boussinesq approximation neglect the density variation if they are not multiply by a factor of greater magnitude for example gravity.

$$\nabla_h \cdot \mathbf{u} + \frac{\partial w}{\partial z} = 0 \tag{2.4}$$

The pressure equation

The pressure equation is used to calculate the last term of the momentum equation (eq: 2.2). It gives the horizontal gradient of pressure considering the hydrostatic approximation meaning that the pressure is only dependent of the height of the liquid above and its density ($p = \rho g h$). The horizontal gradient of pressure will thus be a combination of the horizontal gradient of the height above (which is equal the horizontal gradient of the surface elevation) and of the horizontal gradient of the density.

$$\frac{1}{\rho_0}\nabla_h p = g\nabla_h \eta + \frac{g}{\rho_0}\nabla_h \int_z^{\eta} (\hat{\rho}(S,T) - \rho_0) d\zeta \tag{2.5}$$

Where $\hat{\rho}(S,T)$ is the density depending on the salinity (S) and the temperature (T). It is calculated with the state equation from Jacket et al. (2006) [16].

The salinity and the temperature equations

The salinity (eq: 2.6) and the temperature (eq: 2.7) equations are both advection diffusion equations without a source and without a sink. The red terms in the equations represent the advection and the blue terms represent the diffusion.

$$\frac{\partial S}{\partial t} + \nabla_h \cdot (\mathbf{u}S) + \frac{\partial wS}{\partial z} = \nabla_h \cdot (\kappa_h \nabla_h S) + \frac{\partial}{\partial z}(\kappa \frac{\partial S}{\partial z}) \tag{2.6}$$

$$\frac{\partial T}{\partial t} + \nabla_h \cdot (\mathbf{u}T) + \frac{\partial wT}{\partial z} = \nabla_h \cdot (\kappa_h \nabla_h T) + \frac{\partial}{\partial z}(\kappa \frac{\partial T}{\partial z}) \tag{2.7}$$

Where κ_h and and κ are respectively the horizontal diffusivity and the vertical diffusivity, they are also parameters that are determined by the model chosen.

These 6 equations are the fundamental relations which govern the currents in the ocean. They arise from the Navier-stokes equations under the Boussinesq and the hydrostatic approximations.

Chapter 3

Numerical Model

In order to solve the equations presented in the previous chapter we are going to use a finite element model using an unstructured mesh. The numerical model we chose is the Second-generation Louvain-La-Neuve-Ice-Ocean Model or SLIM.

3.1 The mesh

The first step towards the numerical model is the building of an unstructured mesh. Because the simulation covers an area where the depth exceeds 4000m it is important to work with a 3D mesh. To be build that mesh we will first need a horizontal mesh that will later be extruded vertically.

3.1.1 The horizontal mesh

The horizontal mesh is built using functions included in SLIM. Those functions rely on GMSH a a three-dimensional finite element mesh generator. They allow us to develop an unstructured mesh based on different criteria. But first we need to fix the boundaries of our mesh. Those can be directly drawn on QGIS or set via coastlines that were downloaded.
Once the boundaries set, SLIM can develop a horizontal mesh whose resolution will depend on different criteria such as the bathymetry, the distance towards different interest zone, the distance towards the coastlines and even the error measured from a previous simulation. The model then takes all these different criteria into account to build a unique mesh.

The only limit to the horizontal mesh is the number of elements that are built. Indeed, when constructing the mesh you need to keep in mind that it will be extruded and that therefore each element can be multiplied by the number of vertical layers in the final mesh. You need to limit the number of elements in your horizontal mesh in function of the resources that are available afterwards, when running the model.

3.1.2 The vertical extrusion

In order to go from the horizontal mesh towards a 3D-mesh, we need to extrude the horizontal mesh. That extrusion can be done using z-layers or σ-layers.

Z-layers and σ-layers

The z-layers consists out of horizontal layers parallel to each other and placed at fixed depths. These depths can be chosen through parameters in the model. When extruding the horizontal mesh, if the indicated depth is lower than the bathymetry, then the next element will not be constructed (see fig: 3.1a).

The σ-layers are more adaptive. The vertical distance between two nodes will evolve with the bathymetry. They will be evenly distributed along the vertical axis. Therefore, the different layers will not be parallel anymore (see fig: 3.1b).

There is thus a mesh evolving vertically with fixed distances (z-layers) and another one that will evolve vertically depending on the bathymetry. The distance between two vertical nodes will be a fixed fraction of the total depth at those nodes (σ-layers). The two different types of extrusions are represented on the figure: 3.1.

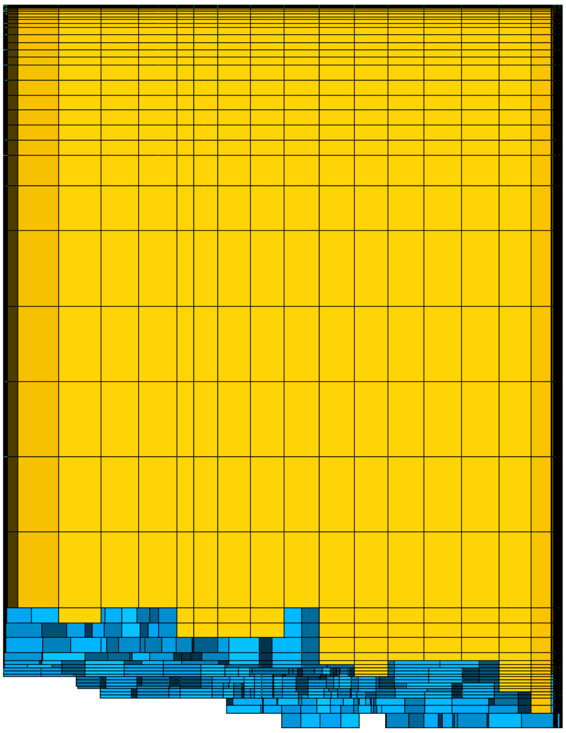

(a) Generating a 3D mesh using z-layers

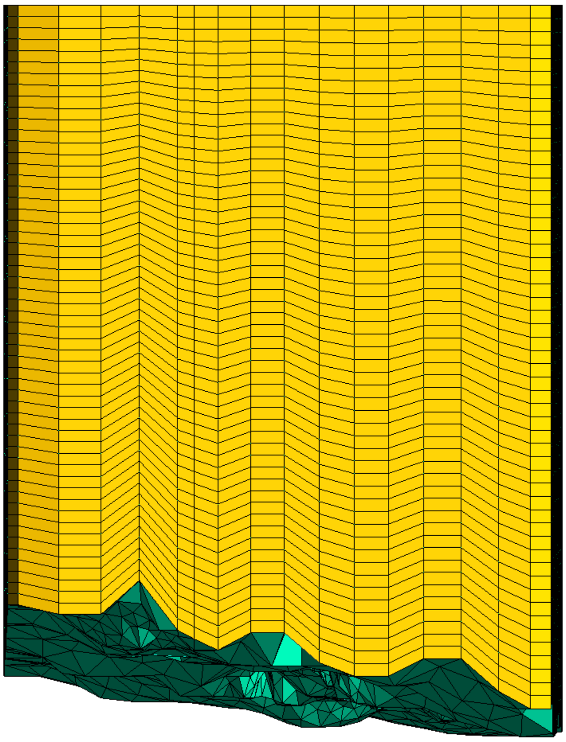

(b) Generation of a 3D mesh with σ-layers

Figure 3.1: Generation of a 3D mesh based on the horizontal mesh. In yellow we have the different layers at a boundary. In blue and green, we see the last layer which will be the bottom of the ocean in our model. It is composed out of step functions for z-layers and out of ramp functions for σ-layers.

The advantages of the σ-layers are the more realistic representation of the bottom of the ocean and the adaptive layers whose resolution can be set more precise near bottom, in the last tenth of the depth for example.
If we want to achieve the same high resolution near the bottom with z-layers we will have to use a lot more layers, it will thus cost us more resources. On the other hand, z-layers are more stable numerically because they do not depend on the consistency criterion.

The consistency criterion

The consistency criterion is a criterion that restrains the use of the σ-layers. Indeed, if the slopes of the bathymetry are too important, that criterion would not be fulfilled leading to hydrostatic errors and thus numerical errors propagating and generating instabilities in the simulation. The consistency criterion needs thus to be fulfilled when we are working with non horizontal grid planes as σ-layers.

If the grid is not flat, the horizontal density gradient will be computed thanks to the vertical density gradient and to the gradient along the grid. That computation may result if the consistency criterion is violated in an inaccuracy in the horizontal density gradient and thus inaccuracies in the currents(see fig: 3.2 & fig: 3.3).

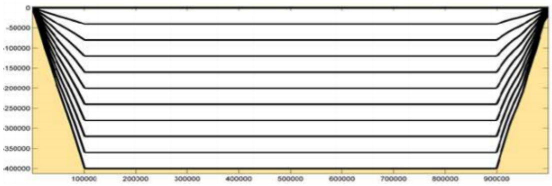

(a) Mesh using σ-layers

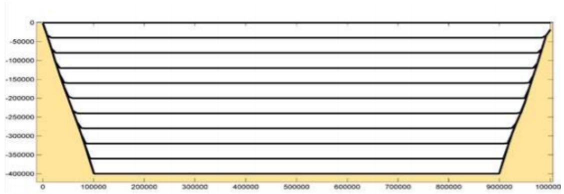

(b) Mesh using z-layers

Figure 3.2: Meshes used for the simulation of the article, note the depth is 1000m – exaggerated x400 for figures. [15]

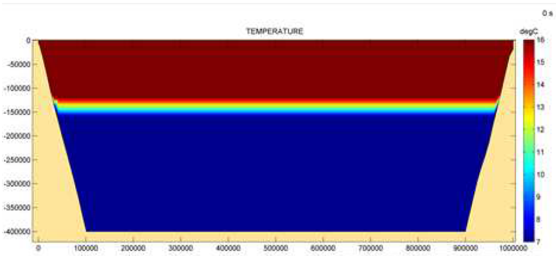

(a) Initial condition (step profile) with flat planes

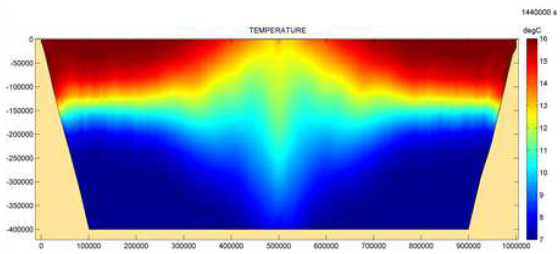

(b) After 17 days initally step density profile with flat planes

Figure 3.3: Evolution of the step density profile with flat planes.[15]

Even the mesh using flat planes will develop some hydrostatic inconsistency flows because the mesh is not totally flat at the edges (see fig: 3.3a). Indeed we observe that after 17 days, the steady initial condition is totally disrupted because of those flows (see fig: 3.3b). That shows how the inconsistency errors can affect our simulation and why it is so important to avoid them. The same phenomenon is also observed with the mesh using σ-layers. In order to avoid the hydrostatic inconsistency errors, the criterion must be fulfilled. In other words, the following equation must be verified:

$$\nabla H = \frac{\Delta h}{\Delta x} < \frac{\Delta z}{\Delta x} \tag{3.1}$$

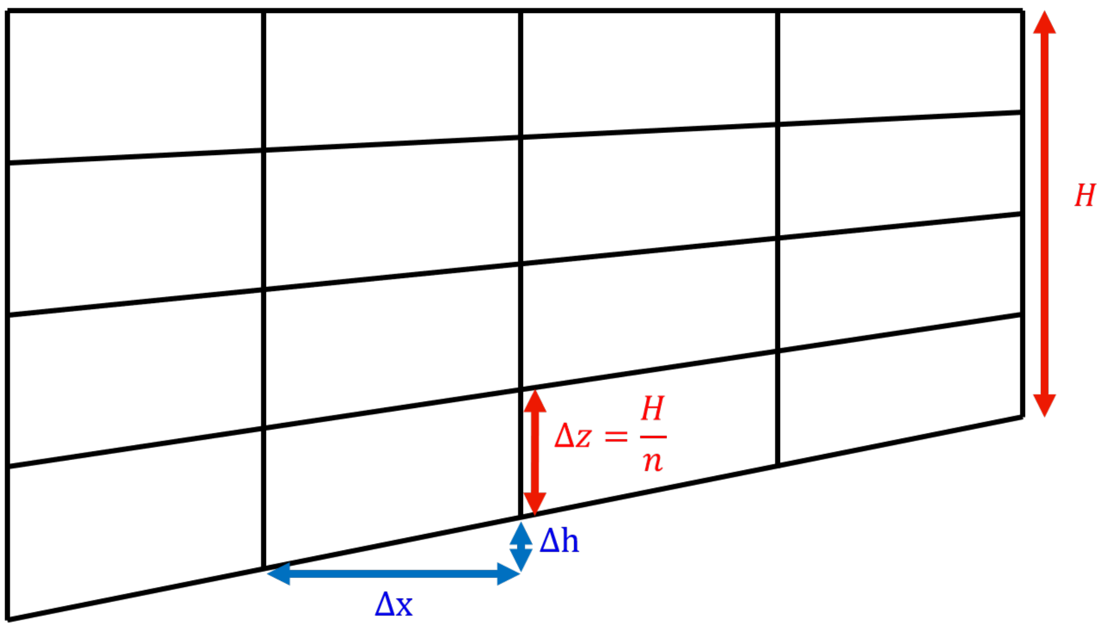

Figure 3.4: Illustration of the different variable of the consistency criterion.

With $\Delta z = \frac{H}{n}$, that gives:

$$\Delta h < \frac{H}{n} \quad (3.2)$$

Where H is the total height where the σ-layers are applied, Δh the difference of bathymetry between two neighboring nodes, Δx the horizontal distance between those nodes and n is the number of sigma layers (see fig: 3.4).

If the consistency criterion (eq: 3.4) is not verified, four options are available:

- We can decrease n to increase Δz. But that will lead to losses in the vertical resolution.
- We can refine the horizontal mesh to decrease Δh (Δx being on both size of the equation the higher resolution will have no impact on it. But if the slope is constant, a smaller Δx will bring a smaller Δh). But a higher resolution will also entail more resources.
- We can smooth the bathymetry in order to reduce Δh. That will make a less realistic simulation, we will lose part of the information of the bathymetry.

3.2 SLIM

Once the mesh built, you need to give initial values to the variables at each node. Then you can use the Discontinous Galerkin method to calculate the evolution of the variables in the time. To do so you need to discretize the 3D hydrostatic equations and then resolve them with a fixed time step in order to simulate the next step. That is what SLIM does. But in order to get there, SLIM need to be initialized, parametrized and the different forcings need to be introduced.

3.2.1 parametrization of SLIM

The parameter used by SLIM are all the different parameters that we set when we wants to start the numerical model. In the equations presented in section: 2.1.1, several parameters were presented. There is the Coriolis factor f, the reference density ρ_0, the horizontal diffusivity κ_h, vertical diffusivity κ, the horizontal viscosity ν_h and the vertical viscosity ν.

- The Coriolis factor is defined in function of the latitude. Indeed it is equal to $2 * 7.292 * 10^{-5} * sin(lat)$. Where $7.292 * 10^{-5}$ is the rotation rate of earth in rad/sec.
- The reference density is set at 1027 $[kg/m^3]$ [16].
- The viscosities and the diffusivities are defined based on turbulent closing of the model. The default turbulent closing used is GOTM (General Ocean Turbulence Model [17]).

In addition to those parameters there are also the parameters linked to our mesh; the boundaries, the resolution and the vertical extrusion. That vertical extrusion needs another parameter, the bathymetry. The bathymetry is mostly provided by GEBCO. GEBCO's resolution is of 15 arc-second intervals or $15/3600°(\approx 450m)$. The grid initially downloaded is from 2019. In addition to that bathymetry, GSR has given us a preciser bathymetry. GSR's bathymetry has got a resolution of 75m horizontally and a range going from 14°N to 14.23°N and from 125.77°W to 126°W.

3.2.2 Initialisation of SLIM

The initial conditions are the values given to the variables in our mesh at the starting of the simulation. We could start the simulation with default values but then the spun-up time of the simulation would be longer. It is thus favorable to initialize the different variables with some initial conditions.

Most of our initial conditions are from HYCOM (HYbrid Coordinate Ocean Model [18]). HYCOM provides a data set on a grid with a resolution of ~ 7 km horizontally. Vertically, HYCOM disposes of 40 levels going from the surface to 5000m deep, the resolution is preciser at the surface and it ends with 1000m between the levels from 3000m depth. The temporal discretization of its data is of 24hours. HYCOM provides our model the initial eastward and northward velocity (u,v), the initial surface elevation (η) and also the initial temperature and salinity (T,S) for the whole domain with which the density can also be found. In addition to HYCOM, OSU TOPEX/Poseidon Global Inverse Solution TPXO7.2 dataset [19] combines different tidal modes to provide additional initial conditions. It will give us an additional velocities (u,v) and a surface elevation (η) linked to the the tidal movement.

3.2.3 Forcings of SLIM

The forcings are the boundary conditions necessary for the proper functioning of the simulation. The four boundaries as a reminder are the following:

- Γ_f, the seabed boundary.
- Γ_s, the surface boundary.
- Γ_n, the lateral boundary.

The boundary condition at the seabed is its impermeability. That means that the flux through the bottom is zero. The boundary conditions at the surface is first the impermeability of the surface but also the wind that creates a stress on the surface that is transformed into velocity. Wind velocities are given by Copernicus climate data store. The resolution of Copernicus' data is of 0.25 degree (≈ 2.775km) and it has a temporal discretization of one hour. The lateral conditions are HYCOM's variables completed with TPXO for the open boundaries and if the lateral boundary is closed then it is the impermeability condition.

Chapter 4

Literature review of the currents and their impact

This chapter will explain the different currents and the ocean dynamics that are expected to be observed in the simulation area. Those are needed in order for us to choose the right parameters and the right forcing for our model. We will thus make a review of the origins of the different currents and evaluate their potential impact in the ocean. When evaluating the their impact, we will focus on the deep-sea. Even if the rest of the ocean is important the main goal is here to develop a good solution mainly for the deep ocean currents.

4.1 Surface currents

There are different surface currents in the eastern pacific. A schematic overview of the ocean currents is presented in fig:(4.1).

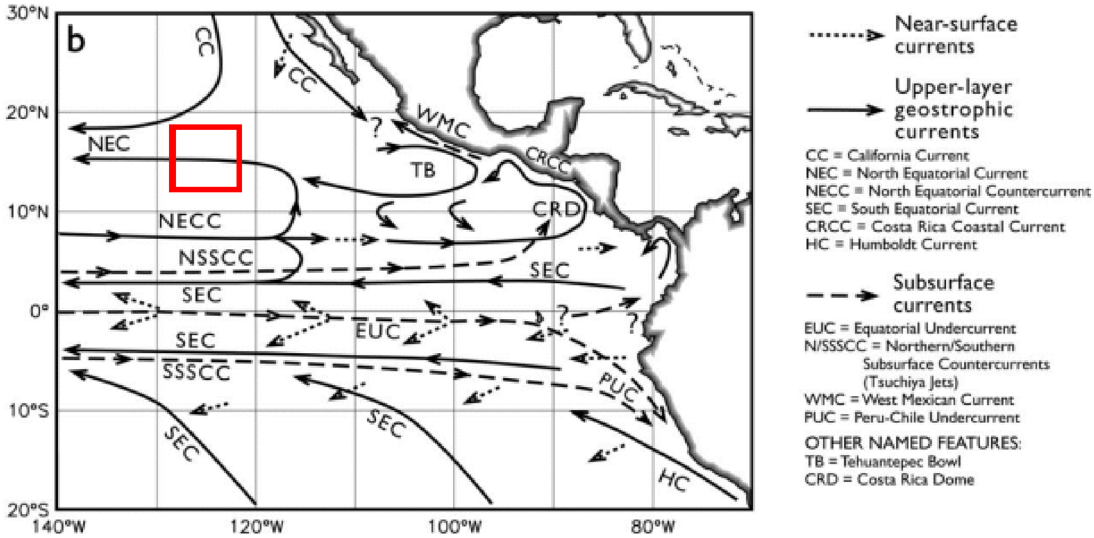

Figure 4.1: Schematic overview of ocean currents around the GSR concession zone (red box).[20]

The main currents around the studied area are the following:

- The North Equatorial current, a westward current that's part of the North Pacific Gyre. The Gyre is a consequence of the coriolis force and is pushed by the trade winds. Its average velocity lies between 10 and 15 cm/sec [?].

- The North Equatorial counter current, a eastward current that stands between the North Equatorial current and the South Equatorial current. It take advantage of a zone where the trade winds are weaker and is created by the NEC and SEC arriving at the American coast. Its mean velocity is of 42 cm/sec.

- The California current is also part of the North Pacific Gyre, it pushes upwelling cold water towards the south. Its common velocity is less than 25 cm/sec.

In addition to those currents, different eddies may reach the concession zone and have an impact on the surface currents. To start, surface currents at the coast of Peru are perturbed by wind jets going through gaps in the mountains. Indeed, lower elevation into the mountains creates gaps where the wind rushes and becomes stronger. The jets then create strong eddies in the ocean. And even if the the jets do not have a direct impact on our zone, the generated eddies might reach our zone and thus have an impact.

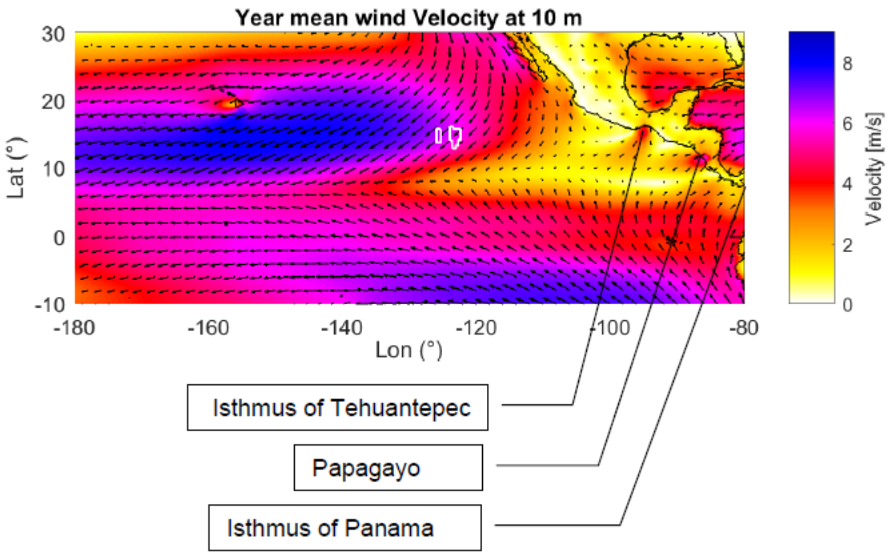

Figure 4.2: Wind jets going through the mountains and generating meso-scale eddies. [21]

In addition to those eddies, the shearing between the SEC and the NECC produces Tropic Instability Vortices. Those vortices will not propagate into our concession zone, but secondary eddies due to them might propagate themselves into the study area.
Those different surface currents will then propagate themselves thanks to the vertical viscosity and influence deep-sea currents. Generally there is a lag of 10 to 12 days between the apparition of those surface currents and their consequences at the bottom of the ocean.

4.2 Deep Ocean currents

Manganese nodules are found in highly stable environment, the deep-sea is there low in energy and speed magnitude are thus low. But that energetic low environment can be very turbulent. Indeed because of the low vertical density gradient, created eddies can last for weeks in the deep-sea. Different factors might be the source of current and/or eddies in the deep ocean, those are represented on fig:(4.4):

- Density driven currents
- Deep water tidal currents
- Internal waves and solitons

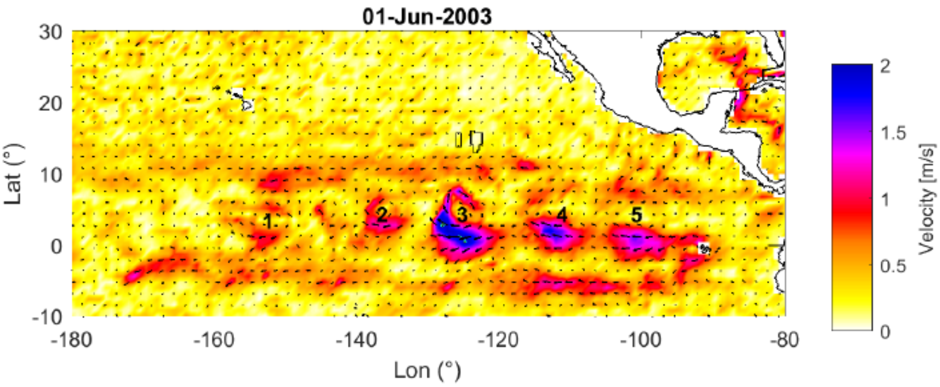

Figure 4.3: Tropical Instabilities Vortices generated by the shear between the NEC and the NECC. [21]

- deep-sea storms
- deep-sea eddies
- Tsunami related traction currents, rogue waves and cyclonic waves.

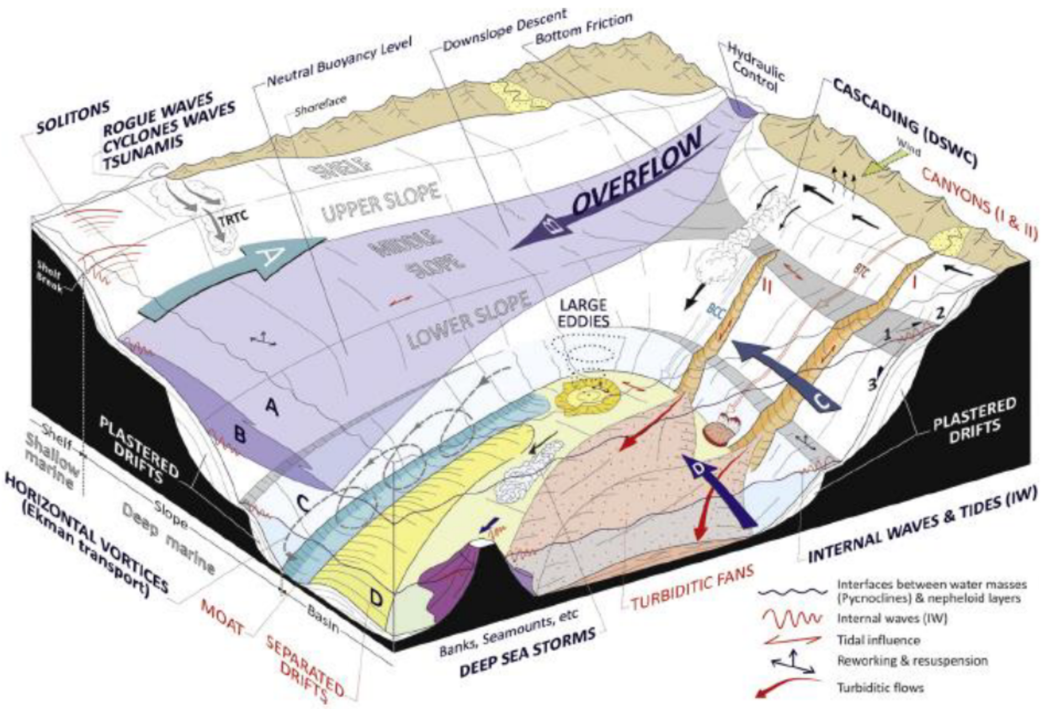

Figure 4.4: Schematic overview of the currents in the deep ocean [22]

4.2.1 Density currents

The density driven current are set in motion by the gravity who acts on the difference of density. The density difference in the ocean is generated by salinity and temperature. Globally, the colder and the more saline, the highest the density will be.

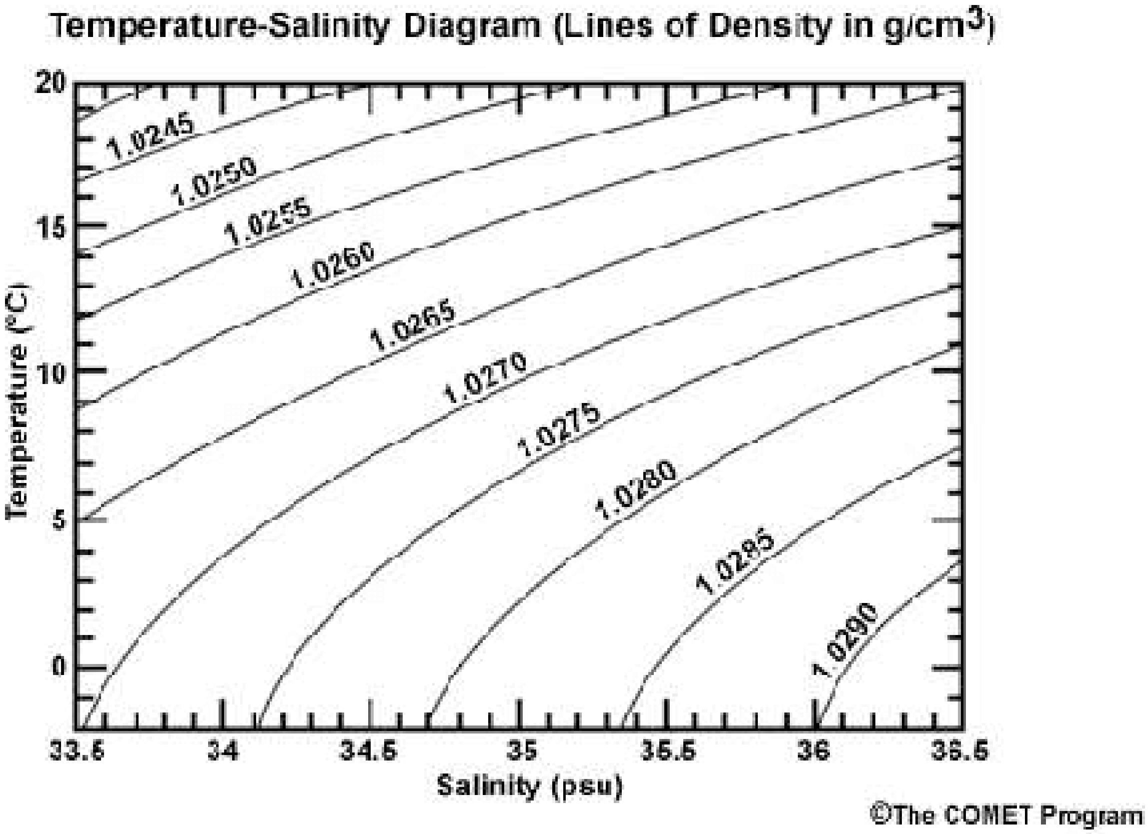

Figure 4.5: water density diagram [23]

thermohaline circulation

The main density current goes around the world is called the thermohaline circulation or global conveyor belt. It's speed is of a few cm/sec and it covers the whole world (see fig: 4.6). It's influence on our zone is however limited: "There are no specific indications that particularly strong density-driven currents occur near the GSR concession area".

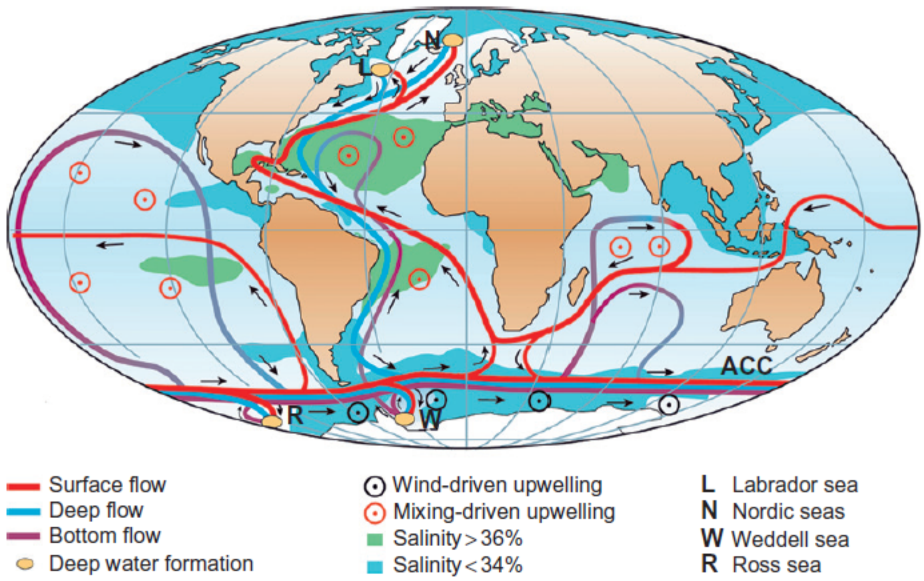

Figure 4.6: The global conveyor belt [24]

Pycnocline

The pycnocline is not a density driven current but it is linked to the density. Indeed a pycnocline is a line that separate two different liquid densities. That line is characterised by a gradient of density. In our zone the pycnocline is majoritarly a thermohaline (gradient of temperature) reinforced by a halocline (gradient of salinity). It lies around 60-80m deep. The pycnocline is a barrier to surface processes. Indeed, because of its stability it tends to block a big part of surface changes keeping the lower layer stable and less sensitive to seasonal changes. It is the limit between surface waters and deep ocean waters.

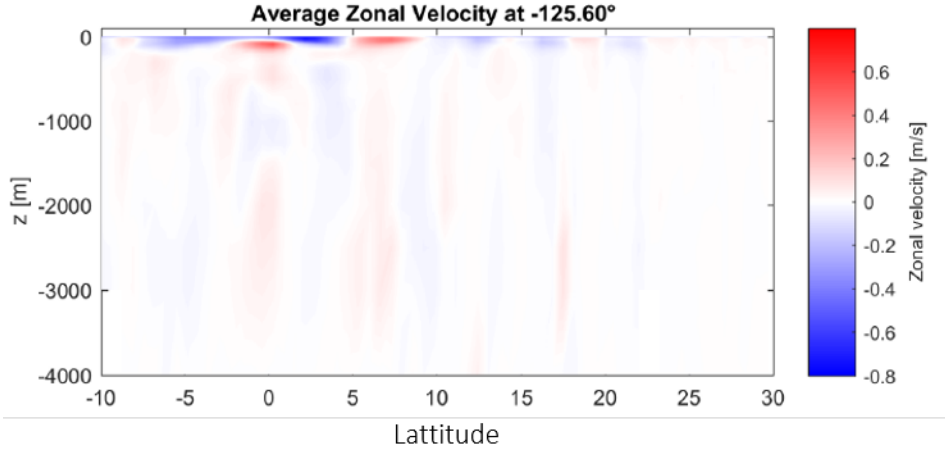

Figure 4.7: Mean average zonal velocity in 1995 at 125.6°W [21]

4.2.2 Deep water tidal currents

Tides may also have an impact on our deep-sea current. The water movement generated by the moon and the sun create baroclinic waves. Those waves interact with the topography and may represent 1/3 of the abyssal current variability [25]. An extraction of the tide fit on collected data confirms the influence of tidal generated currents (see fig:(4.8)). Even if the fit is only of few cm/sec, the magnitude in the deep-sea are supposed to be really small and it can thus represent a big part of the deep ocean current.

4.2.3 Internal waves and solitons

Internal waves and solitons are waves propagating at non tidal frequencies. They advance along a density gradient as the pycnocline. But there are no trace of big impact of internal waves around our zone.

4.2.4 Benthic storms

Benthic storms occur when the current velocity raise above a certain limit. The shear stress provoced by the the current will then generate plumes resuspension. They may appear in our zone. Current are then rising up to more than 13cm/sec [21]. The storms can happen during a period up to 10 days. Those phenomenon are still poorly understood, but they seem to occur in regions with high eddy kinetic energy and they seems to be linked with meanders, rings, typhoons or fast moving hurricanes.

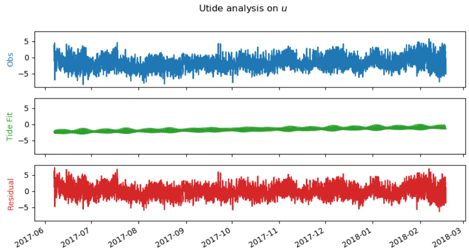

(a) Tidal fit for u 3.46m above the seabed

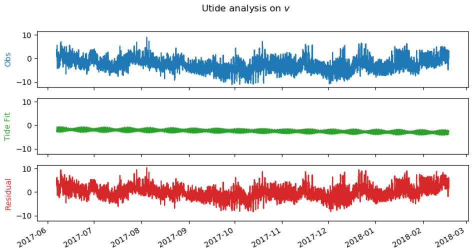

(b) Tidal fit for v 3.46m above the seabed

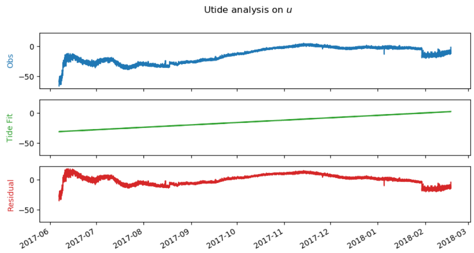

(c) Tidal fit for u 15.46m above the seabed

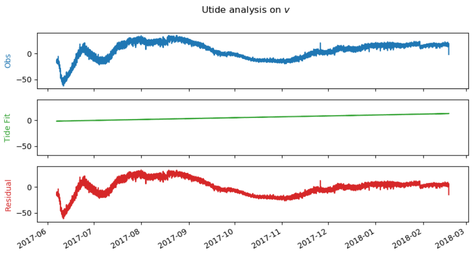

(d) Tidal fit for v 15.46m above the seabed

Figure 4.8: Tidal extraction of collected data at Mooring 04 (velocity in cm/sec)

4.2.5 deep-sea eddies

deep-sea eddies find they origin on two places. First they can be a consequences of surface eddies generated by the wind (if those are really high they can start a benthic storm), those surface eddies were already discussed previously.
On another hand they can be formed due to the interaction of the current passing by ocean seamount. Those eddies are not perceived by Hycom. The different eddies might also bounce into each other being destructive or constructive and having thus more or less impact.

4.2.6 Tsunami related traction currents

The tsunami related traction currents are considered to be too episodically and too short to be really taken into account. Also their real influence is more in shallow waters.

4.2.7 Literature review conclusion

After reviewing the different factors that could affect the deep-sea currents, we note that they are three main driving factors that could affect the dynamic of the deep-sea. It is therefore to these that we must pay the most attention to when building our model.

- The tidal movement.
- Deep-sea eddies formed by the wind.
- Deep-sea eddies from seamounts.

Chapter 5

Results

5.1 Building the mesh

5.1.1 Building the horizontal mesh

The mesh developed has the same geographic boundaries used by the GSR. The mesh went from 127.92°W to 121.2 °W and from 11.28°N to 17.92°N. It is 732km wide and 738.3km long (see fig: 5.1a). This amplitude is needed in order to take into account the impact of the wind and the seamounts on the deep-sea currents which are essential as seen previously.
Secondly we need to choose the resolution of the mesh. Because our focus is to arrive at a realistic hydraulic simulation, we chose to make the resolution evolve in function of the distance from the Mooring04. We want the best precision near the Mooring04 in order to compare afterwards the results of the simulation to the collected of the mooring04. The evolution of the resolution in function of that reference point is the following; At less than 10 km from the mooring the distance between two nodes is of 1 km. Then it increases linearly to 4km when the distance reach 30 km. Finally the distance between two nodes reach 40 km when they are further than 225 km from the mooring[1]. We are also looking for a sharper resolution near the seamounts[2] to include their perturbations in the simulation. So we added a dividing depending on the distance from any seamounts and from the mooring. If the point is at less than 250km from the mooring and at less than 1km from a seamount, the dividing factor is 15. Further from the seamount, the dividing factor increase linearly to 1 when the distance from a seamount reach 5km. For a distance between 250km and 500km from the mooring, the dividing factor is

[1]Ideally, it is better to have a resolution at the borders of the same magnitude as the forcing ($\approx 7km$ for HYCOM) to avoid any loss of information.

[2]Seamounts were defined as points on the grid where the bathymetry was shallower than 4000m.

5 and it evolves as the previous dividing factor. For a distance higher than 500km, the dividing factor is 5 and it evolves like the previous two dividing factors.
We chose the different parameters that defined our resolution in order to have a smooth evolution of the resolution while keeping it refine near the mooring04 and the seamounts and keeping the number of triangles below 2500. That limit was set to avoid needing too much resources afterwards.

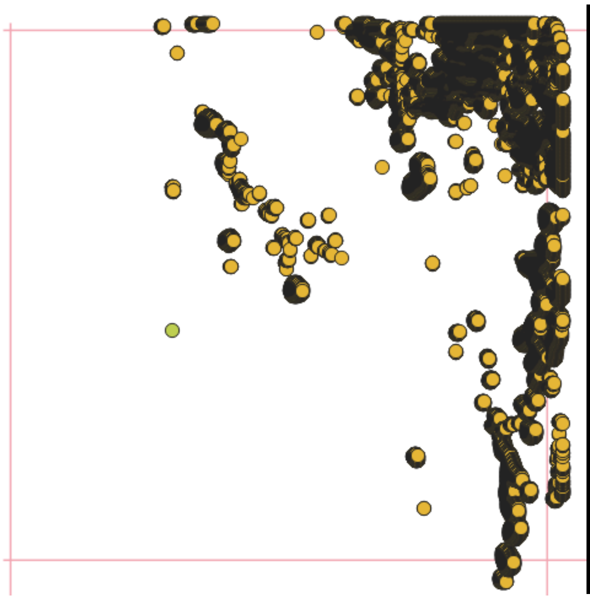

(a) The boundaries are in red, the interest zone (Mooring04) in green and the seamounts in yellow

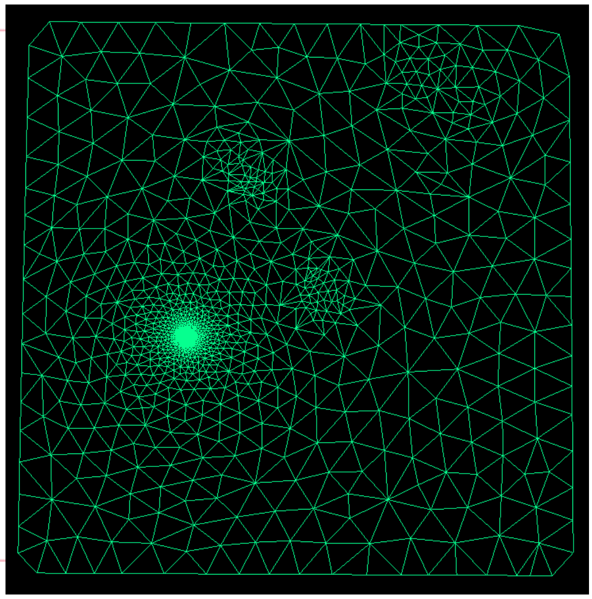

(b) Mesh generated with a refinement around the mooring04 and the different seamounts. The mesh is made of 2348 triangles and 1208 nodes.

Figure 5.1: Building the mesh

5.1.2 Extruding the horizontal mesh

When extruding the horizontal mesh we wanted to work with σ-layers in order to have a high precision near the seabed without using too mush resources. But that high resolution with the sigmas is not fulfilling the consistency criterion (see fig: 5.3). So we consider the different options presented previously and we looked at the bathymetry crossed to our horizontal mesh.

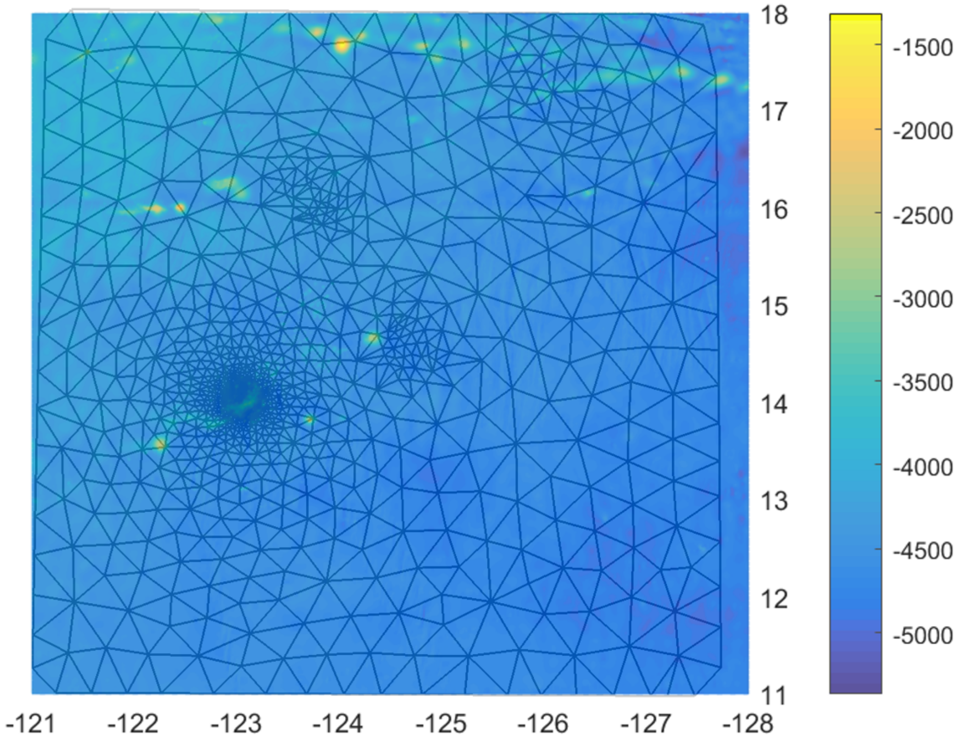

Figure 5.2: Overlapping of the bathymetry from GEBCO and our mesh[26]

Two things can be noted; First The distance between two nodes is very large far away from the mooring04, a maximum distance of 40km. There a smoothing will have no real effect on the criterion unless the smoothing factor is really high. But a really high smoothing factor will result in a big loss of information.
Then there are some big differences in the bathymetry due to seamounts. The span of the bathymetry goes from 1312m to 5366m depth. There is thus a possibility for big differences between two nodes of the same element and thus a possible problem with the consistency criterion.

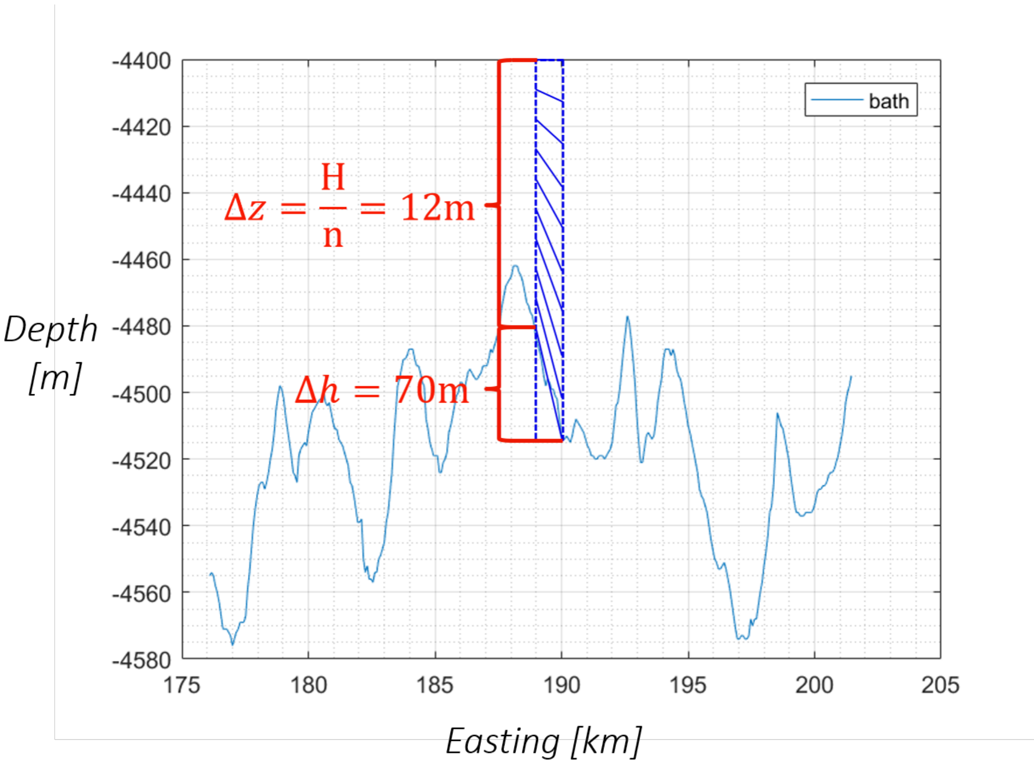

Figure 5.3: Illustration of the consistency criterion unfulfilled around the Mooring04 at latitude 14,16°N

So to avoid the consistency criterion problems we adapt our vertical mesh in two stages. First, we extrude our horizontal mesh by using a two-fold (three) $\sigma - coordinate$ system. That system divides the extrusion in different parts. z-layers are used above 4400m and under 4600m depth and between those we use 10 σ-layers dispatched between 4490m until 4600m (or the bottom of the ocean). The sigma layers are set only if the bathymetry is deeper than 4450m depth. Doing so we only need to focus on steep bathymetry between 4450m and 4600m (see fig: 5.4).

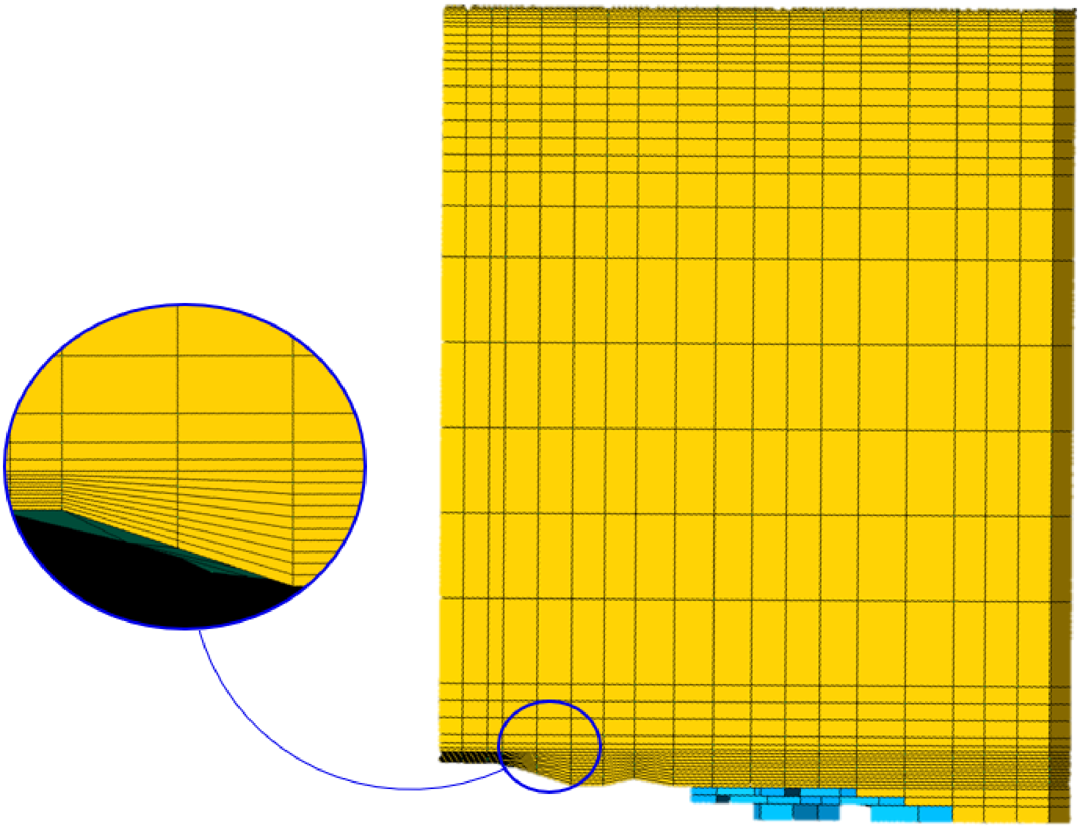

Figure 5.4: Zlayers and sigmas mixed in a three-fold $\sigma - coordinate$ system [?]. The top layers are tightened in order to transmit the surface eddies towards the bottom. The bottom layers are tightened to enhance our precision there. There are a maximum of 51 vertical layers which create a total of 53 666 nodes.

But with only that solution, the code is not stable yet, the consistency criterion is still not verified. So we change the bathymetry away from our focus zone (outside the high resolution bathymetry of the GSR). There we use a step function to force the bathymetry to 4400m or 4600m when its value is in between them. And near the mooring04, into the high resolution zone we make a smoothing of the bathymetry based on lucy's kernel function with a radius of 5000m (see fig: 5.5). Doing so we avoid a big part of the hydrostatic errors linked to the hydrostatic criterion.

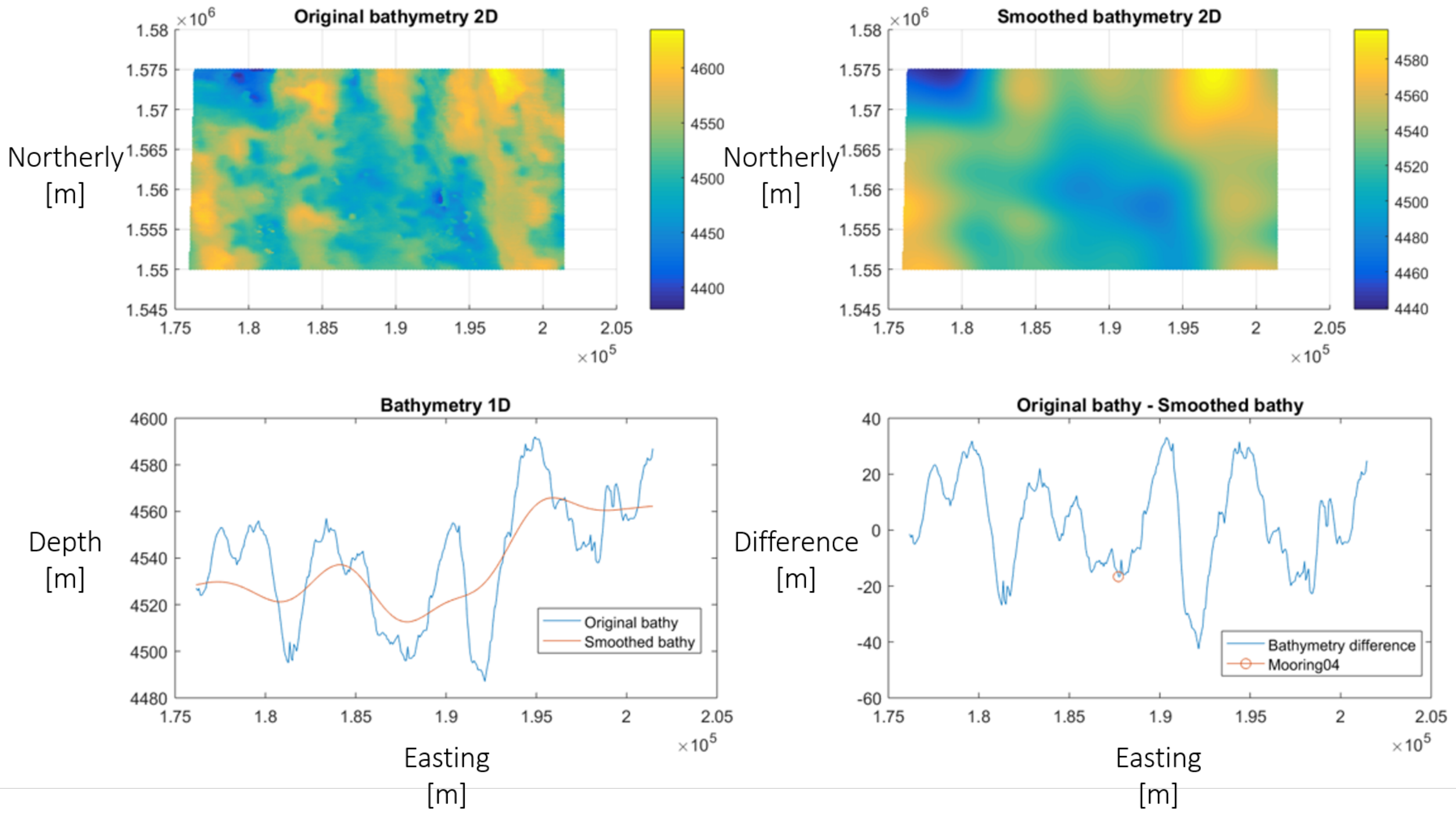

Figure 5.5: Smoothed bathymetry illustration in 2D (two images from above) and in 1D (two images from below) at latitude 14.16°N

5.2 Building SLIM

The parametrization being defined in section: 3.2.1, we only need to set our initial conditions and our boundary conditions in order for our model to run.

Choosing the initial conditions

The initial conditions are based on HYCOM and TPXO as we saw previously. But when preprocessing HYCOM's data, the low resolution at the bottom of the ocean generated some errors. Indeed, HYCOM gives no value between 4000m and 5000m depth. So if our bathymetry is less than 5000m deep, we will have no value given by HYCOM for the nodes under 4000m. The temperature and the salinity will thus evolve to a default value. In order to avoid that and to stay as realistic as possible, we force the salinity and the temperature given by HYCOM at 5000m deep and we make it equal to the ones at 4000m deep. Doing so we avoid the errors.

Choosing the forcings

The forcings were also seen previously. But we decide not to use the forcing linkes to the salinity. Indeed, because the pycnocline is mostly a termohaline reinforced by a halocline, we will assume the salinity constant as set in our initial conditions. That will remove the salinity equation and simplify the model thus freeing some resources. The velocities on the contrary are kept, and their mean magnitude during the simulation is plot here under.

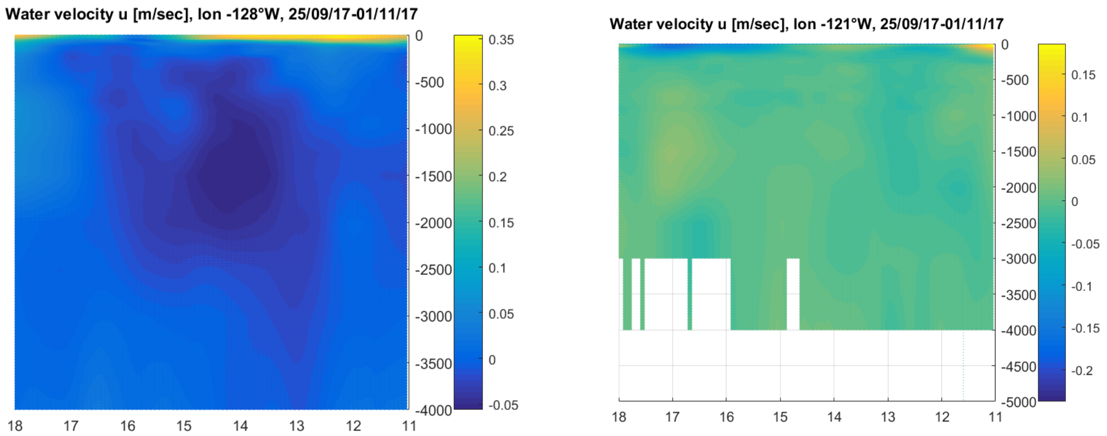

(a) Water zonal velocity on the west border

(b) Water zonal velocity on the east border

Figure 5.6: Zonal velocity on the east and west border in function of the depth (positive is east to west)

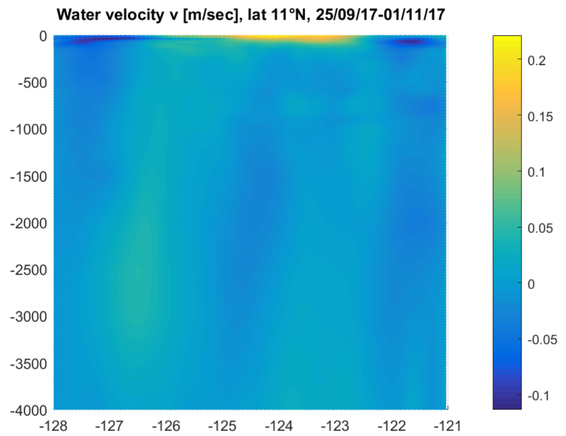

(a) Water meridional velocity on the south border

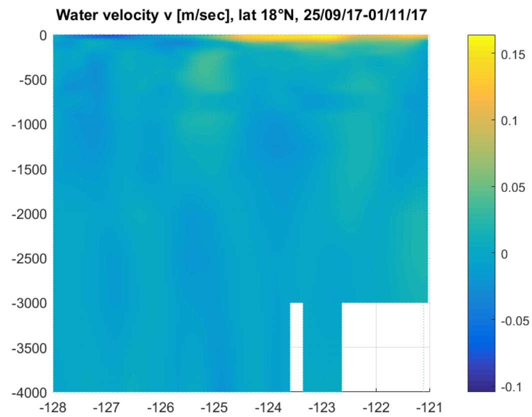

(b) Water meridional velocity on the north border

Figure 5.7: Meridional velocity on the North and South border in function of the depth [m] (positive is east to west)

We observe that the magnitude of the velocities are really low deeper than 500m. We can also observe the lack of information of HYCOM. Indeed there is no data under 4000m deep.
There is also a mismatch between our mesh resolution at the borders and HYCOM's resolution. Indeed the resolution at the borders of or mesh are greater than HYCOM's horizontal resolution. Our mesh will thus not be able to capture the total amount of data provided by HYCOM. But given the limited resources it is necessary to limit the precision of our mesh at the borders. Another forcing that provides some velocity and a surface elevation on our lateral borders are the tides. They are directly incorporate into the model thanks to TPXO. The surface boundary will have as forcing the wind. It is supposed to have great influence. Here are the forcing imposed thanks to CDS:

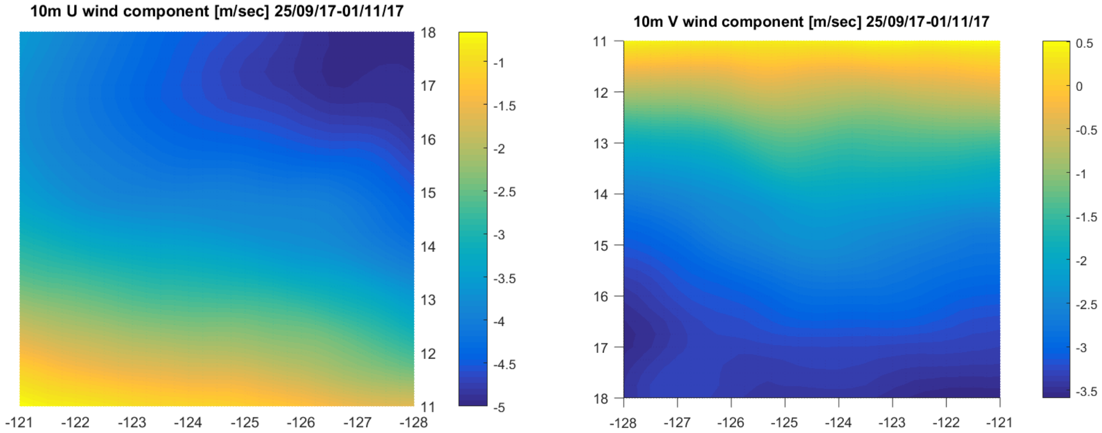

(a) wind u component mean 25/09-01/11

(b) wind v component mean 25/09-01/11

Figure 5.8: Wind forcing

We observe that the mean direction of the wind seems to be the North-East with a marked tendency towards the east.

5.3 Simulation results

5.3.1 The resources needed

During the whole thesis we are try to limit the resources needed by the simulation. That is because the simulation runs on the CECI (Consortium des Équipements de Calcul Intensif) cluster Lemaitre3. The CECI is a consortium that gathers different supercomputer centers from universities in Brussels and Wallonia. These supercomputers can then be used and their power is distributed evenly between the users. There is thus a priority ranking who is build in function of the resources already used. In order to run multiple simulations and to avoid losing too much priority, it is thus important to limit the resources used.
We are working on Lemaitre3, a cluster of the CECI. Lemaitre3 is a cluster who features 80 computer nodes with two 12-cores Intel SkyLake 5118 processors at 2.3 GHz and 95 GB of RAM (3970MB/core). It is best suited for parallel jobs.When running our simulation, we are using a time step of 5seconds to keep the simulation stable and we are exporting every hour. The resources used to simulate the model from the 25 of September until the 31 October are 8 nodes with 16 task per node so we are using a total of 128 processors. Each of them is using 3000mb. And with those resources the supercomputer needs around 1 day and 11hours to finish the whole simulation. Lemaitre3 can have simulations running for maximum two days.

That is why we try to limit the resources used and needed.

5.3.2 Mooring04 data

In order to verify the results of our simulation, we will compare them with the collected data from the GSR. The comparison is done on the mooring04. The mooring04 collected data from June 2017 until March 2018 (see fig: 5.9). It has collected data for different heights above the seabed ranging from 3,46m to 15.46m.

The focus is set on 3.46m and 15.46m above because they are the two limit heights. We limit the amount of graph shown for the sake of clarity. Because the simulation runs from the 25^{th} of September 2017 until the 31 of October 2017. We will zoom on the collected data in order to be able to compare them with the simulations (see fig: 5.10).

The orientation of the current is globally oriented to the South and there is no clear Eastward or Westward orientation. Also, there is a big velocity difference between near bottom currents and the currents at 15m high above the seabed. Indeed, the velocity at 3.45m is around 5cm/sec and at 15.46m it is around 15cm/sec. We can assume that the big difference between the currents and the variation in the East-West orientation is due to highly turbulent nature of the deep-sea.
We also note that the current velocity seems a little high. Indeed, based on the literature we were expected currents with a velocity around 8cm/sec [11] [25] unless there is a benthic-storm. But the persistence of the high velocity tends to show us that the high velocity is not due to a benthic storm (As a reminder, a benthic storm last for about 10 days).

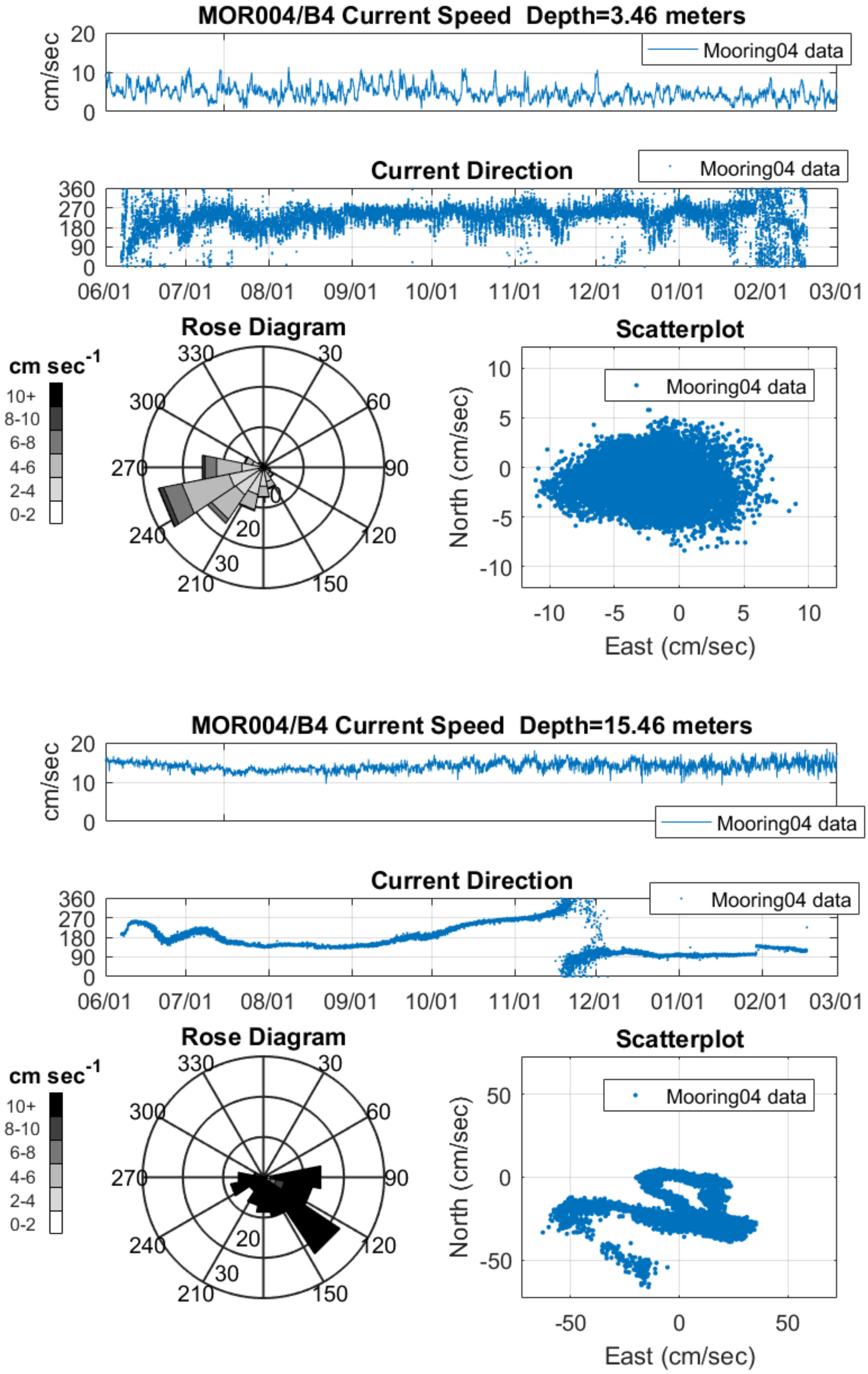

Figure 5.9: Original current measures at mooring04

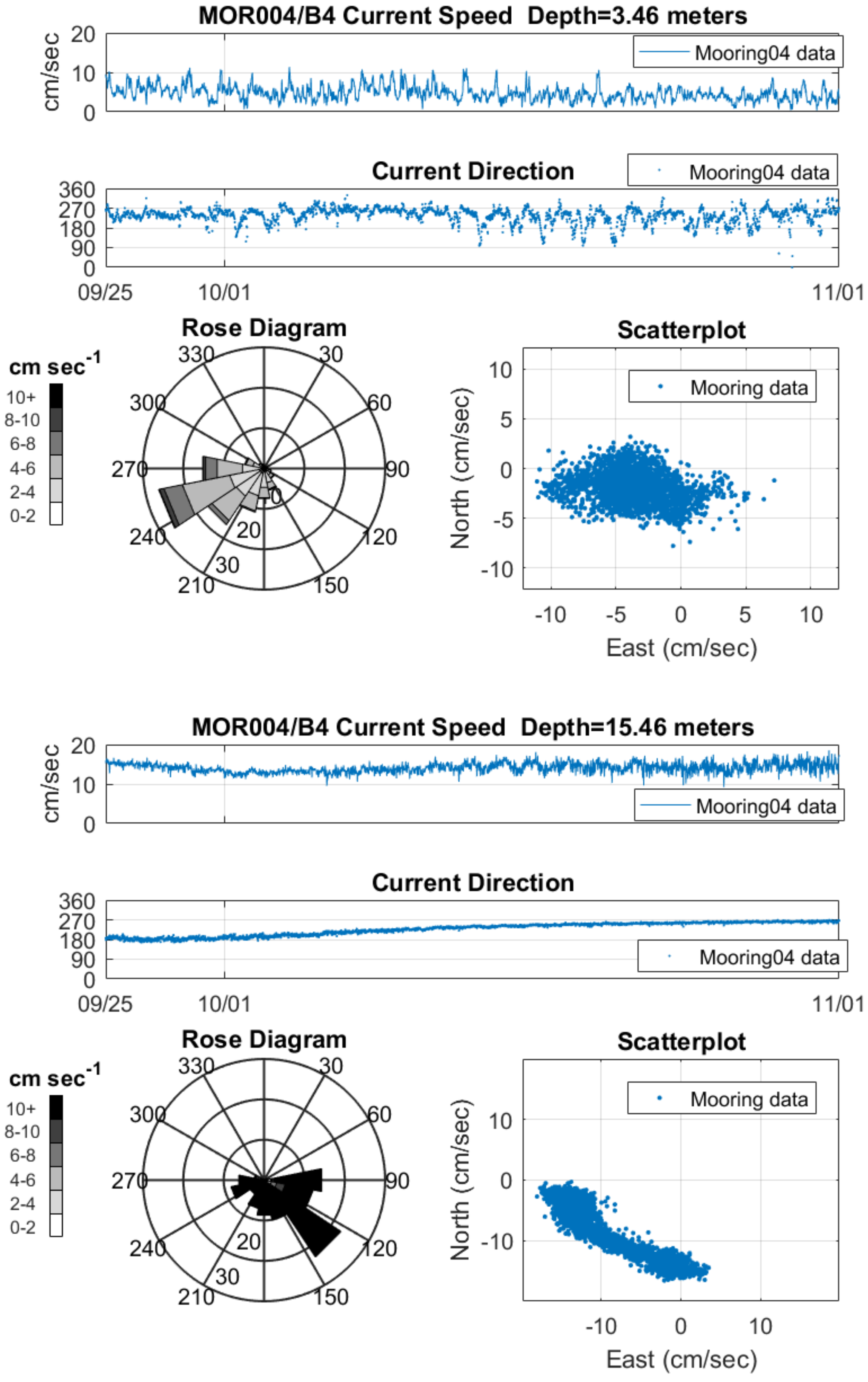

Figure 5.10: Zoom of the current measures at mooring04

First simulation with SLIM

The first completed run that was achieved with SLIM3D on the right temporal scope had as horizontal mesh the one presented in the section: Building the mesh. It was extruded following the three fold σ-coordinate system (see fig:5.4). With the large bathymetry stagered to 4400m or 4600m and the detailed bathymetry smoothed with lucy's kernel function and a radius of 5km. The time step used is of 5 seconds and the data are extracted every hour.

In comparison to the data collected by the GSR, we observe that the velocities obtained are too low. Around 2 cm/sec at 3.46m above the seabed as well as 12m higher (see fig: 5.12). Also there is almost no difference between the heights as well in terms of current orientation than in terms of speed magnitude. It seems thus that our model do not bring enough energy towards the bottom of the ocean.

One possible reason for that is that the vertical viscosity is not sufficient to bring the surface energy towards the bottom. As a reminder, the vertical viscosity is set by default with GOTM. When plotting the vertical viscosity, it showed that the vertical viscosity was at its minimum value of 10^{-6} everywhere under 20m (see fig:5.11).

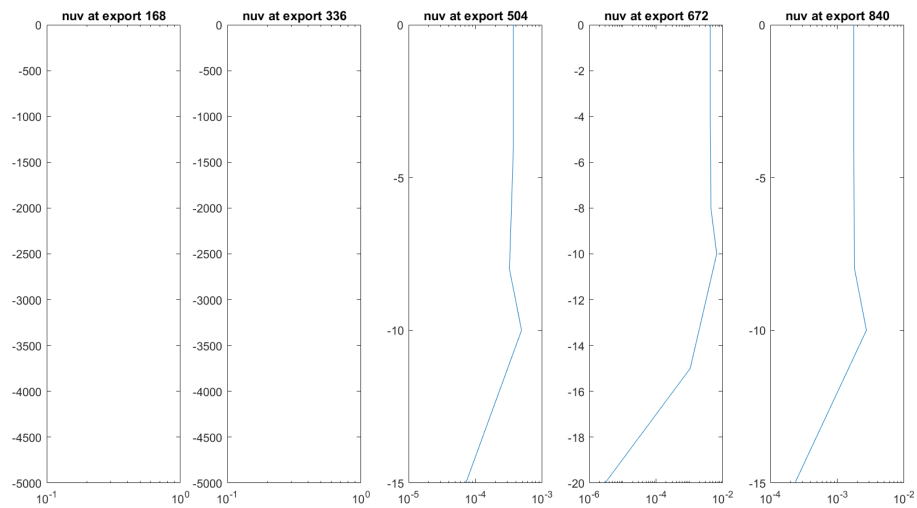

Figure 5.11: Evolution of the vertical viscosity before adding the default minimum value. The plot shows the 5 first weeks of the simulation.

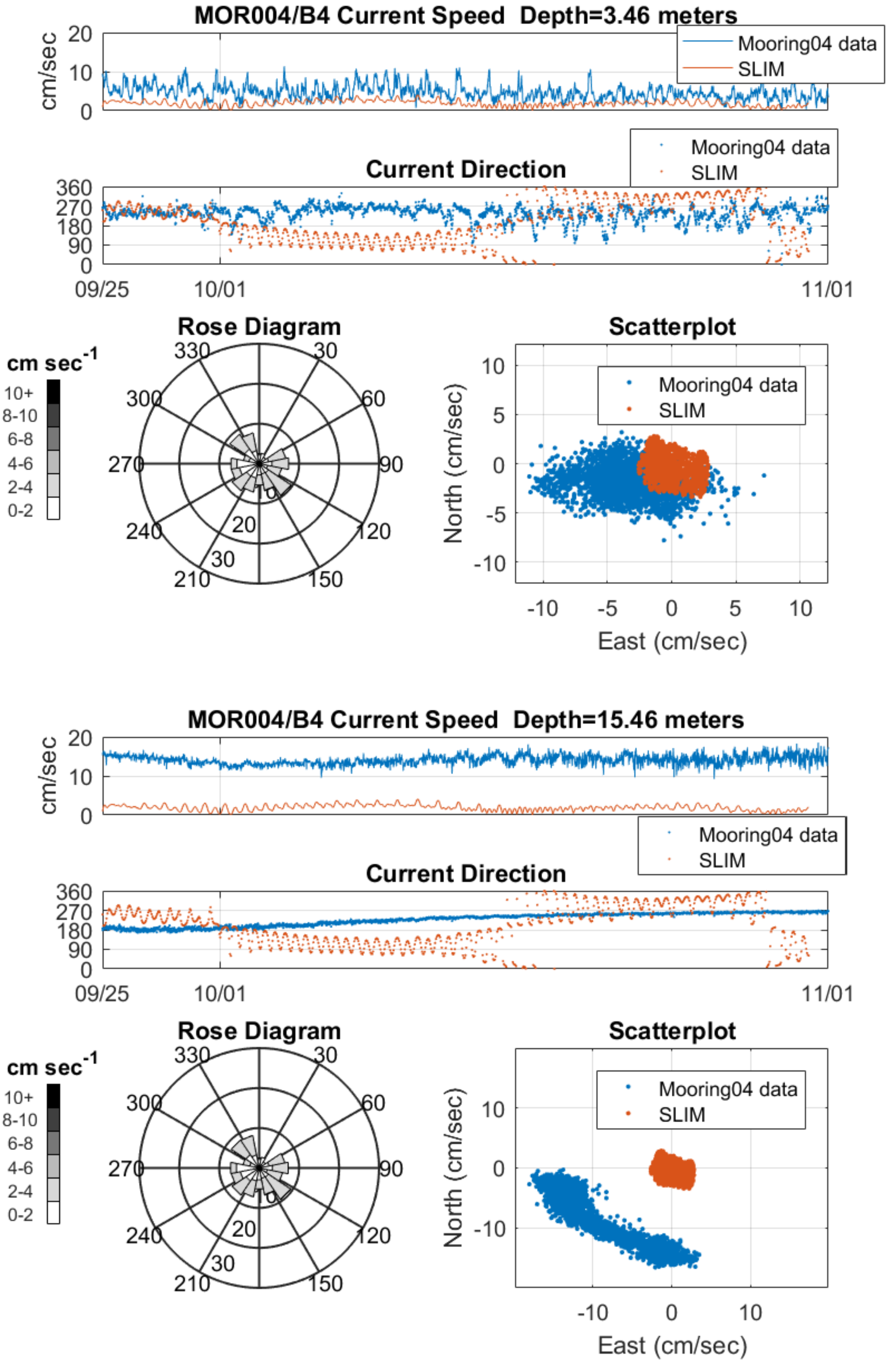

Figure 5.12: First simulation results at 3,46m and 15,46m above the seabed

Second simulation with SLIM

To ameliorate the preceding result we changed the default minimum value of the vertical viscosity to $5e^{-3}$. Unfortunately there was almost no difference with the precedent simulation (see fig: 5.13).

Third simulation with SLIM

In order to adapt and to obtain a greater velocity in our simulation at the bottom of the ocean we changed the whole turbulent closer model. We changed the default closure, GOTM to a new one more adapt to deep-sea and oceans. The new closure is Pacanowski and Philander's turbulent closure model, it will change the vertical diffusivity and the vertical viscosity. The results were better but the velocity is still too low at 15.46m above the seabed (see fig: 5.14).

Fourth simulation with SLIM

All our velocities being too small compared to the data of the GSR, we were wondering if the data collected were not incorrect. Indeed, during the literature review we noted that the velocity expected was supposed to be around 8cm/sec or lower.
So we tried a new simulation on another mooring with other data. There the collected velocity was lower, and thus the results were closer, at least for the speed magnitude (see fig: 5.15). But the orientation of the current is totally Eastward contrary to the data where the orientation is totally mixed (see fig: 5.15 & fig: 5.16). The results are thus here again not conclusive.

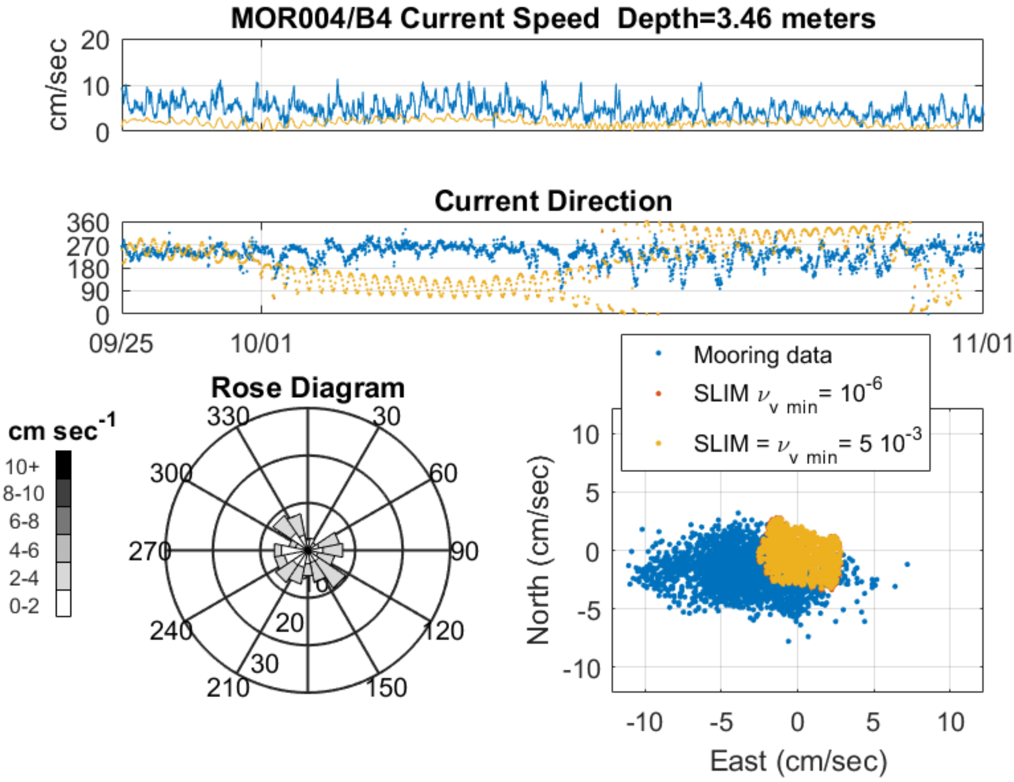

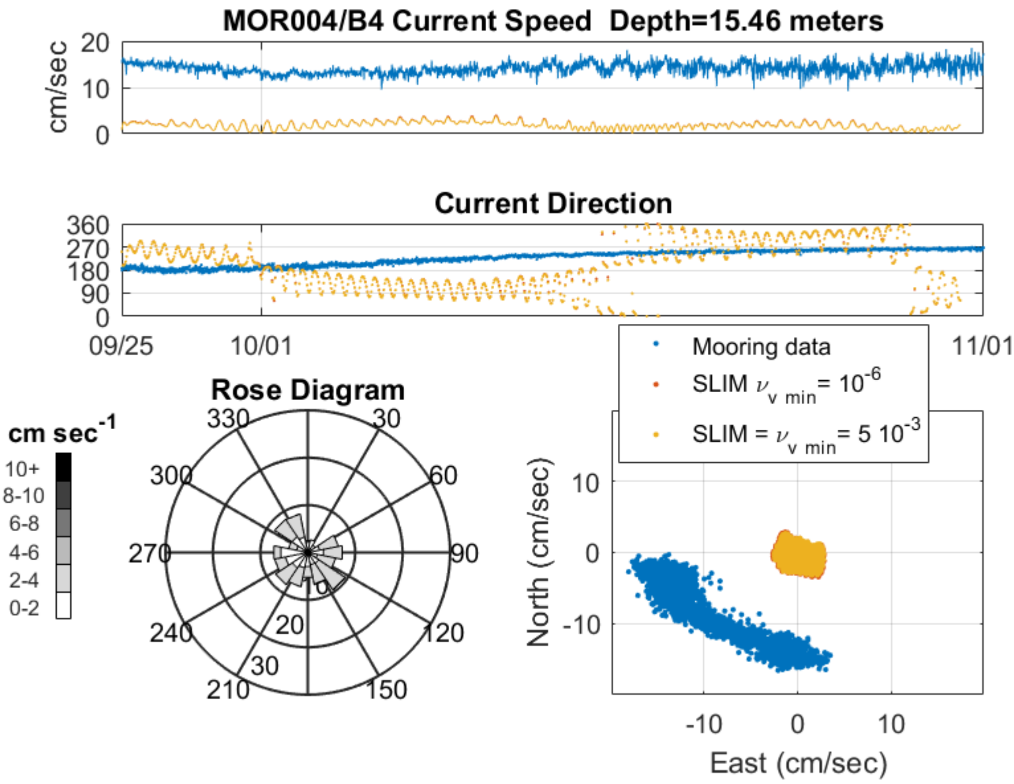

Figure 5.13: Second simulation results at 3,46m and 15,46m above the seabed

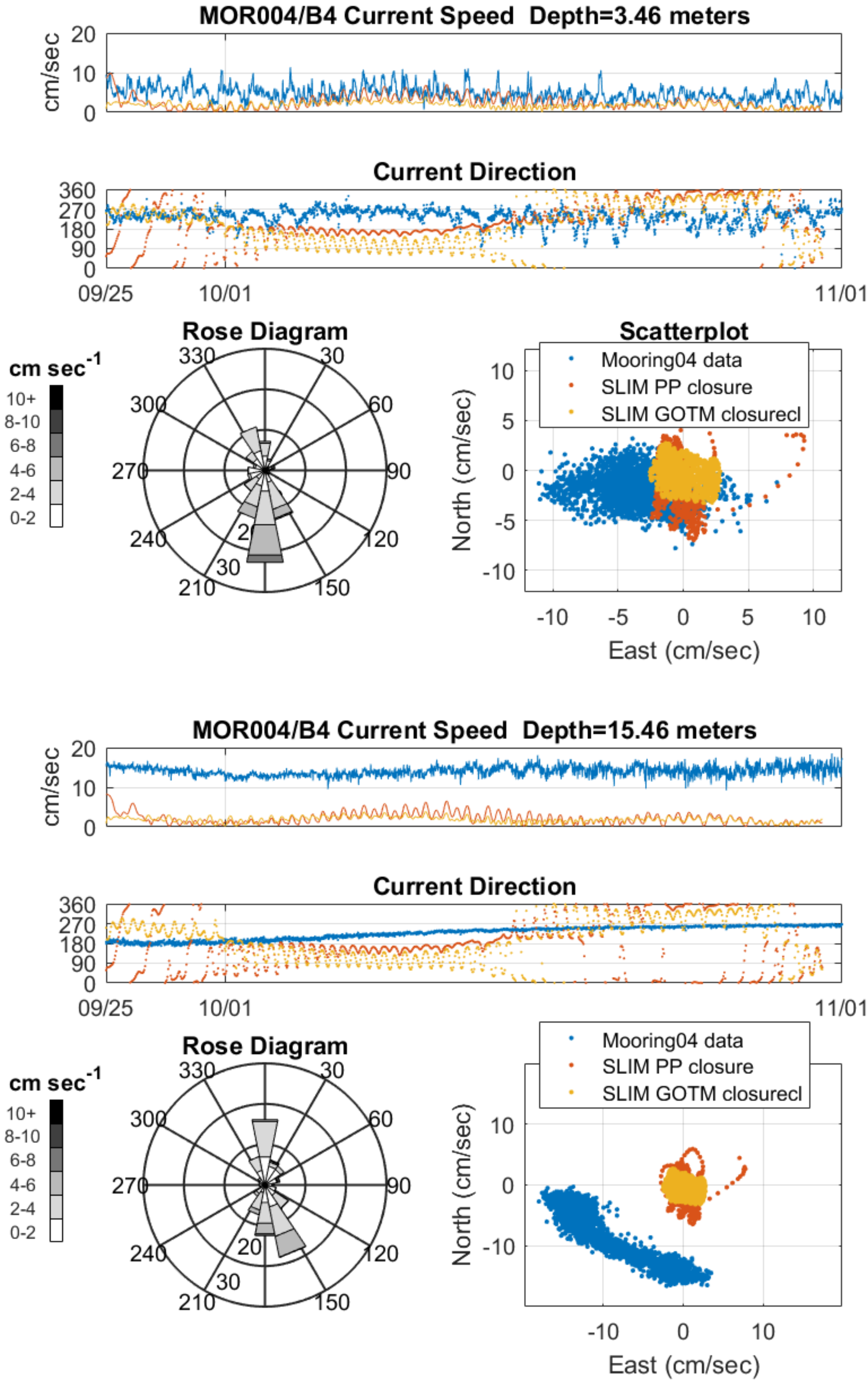

Figure 5.14: Third simulation results at 3.46m and 15.46m above the seabed

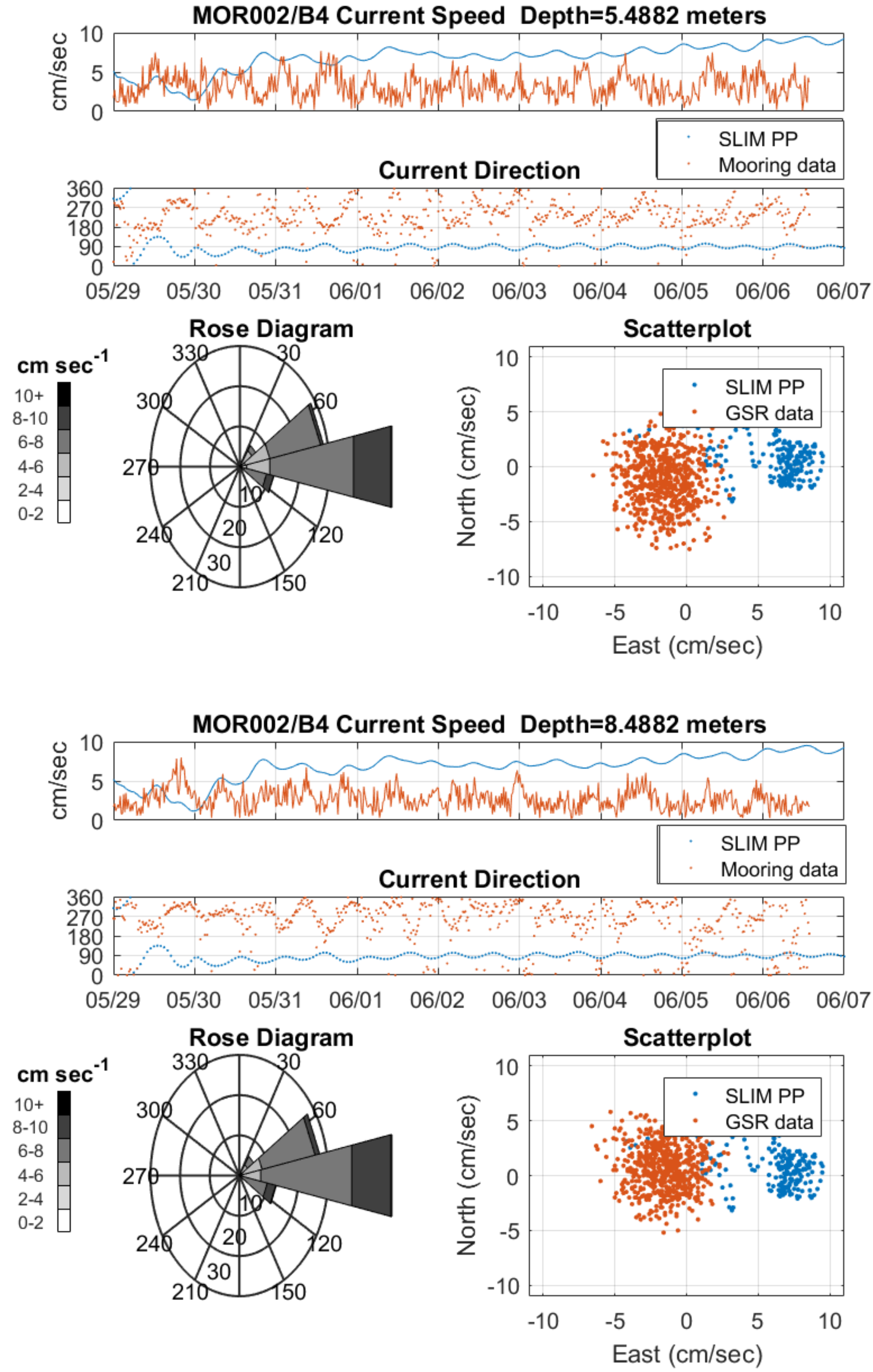

Figure 5.15: Fourth simulation with results at 5.5m and 8.5m above the seabed

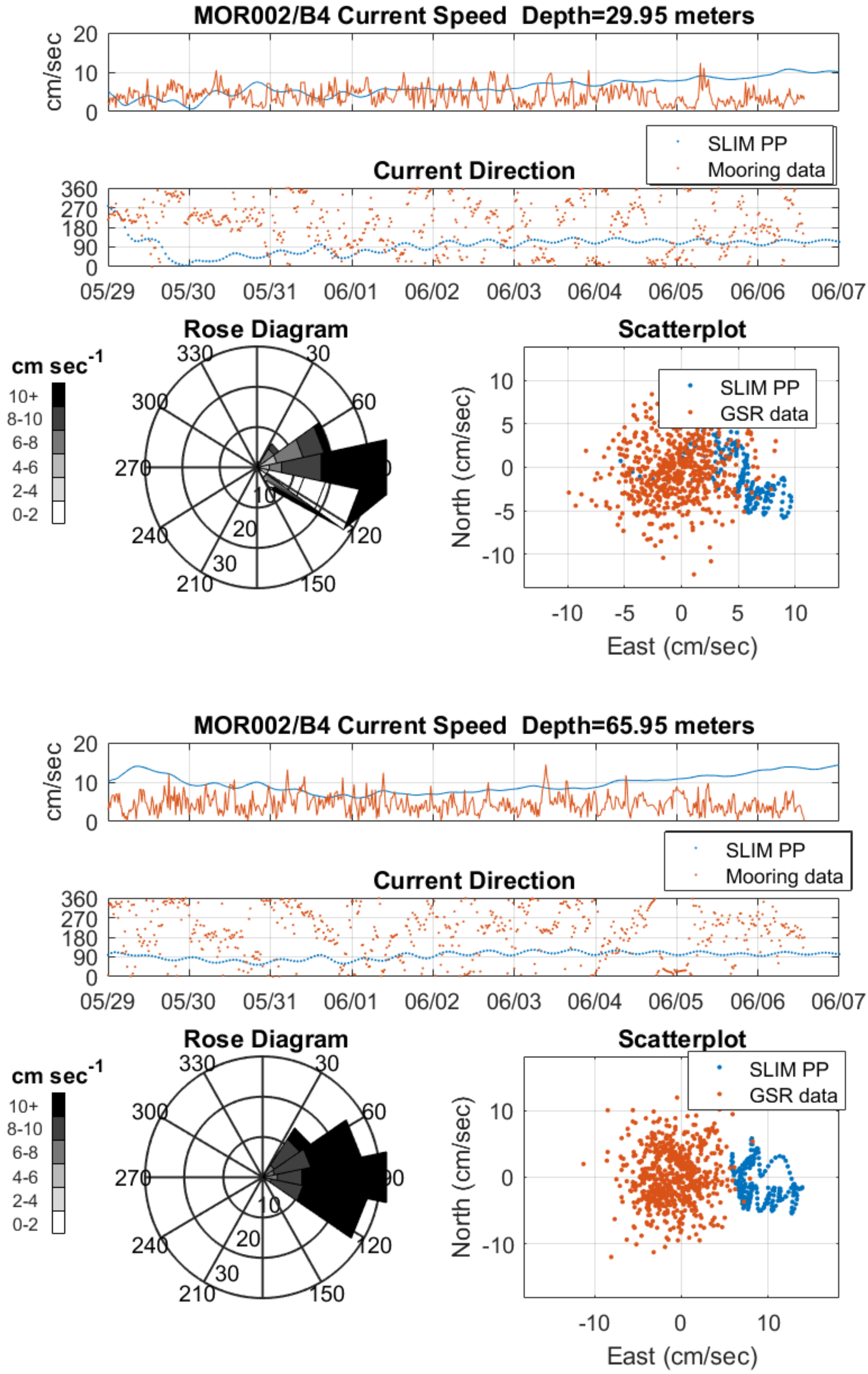

Figure 5.16: Fourth simulation with results at 30m and 65m above the seabed

5.3.3 Discussion

The different simulations presented here above have no real convincing results. Indeed the currents magnitude are for the mooring04 way too low and for the mooring02 they are totally in the wrong direction. There is thus somewhere in our model some gaps who are preventing us from having a match between the collected data and our results.
Those gaps may come from the coarse resolution of our forcing (HYCOM) near the bottom of the ocean. Often, it will only give us the velocities up to 4000m depth. And above 4000m the data are given at 3000m. The grid is thus really coarse and may miss to force part of the ocean deep-sea dynamic.
Another potential reason that could explain the differences is the coarse resolution of our horizontal mesh that has got a distance of 40km between two nodes. This distance may be too high for the model to capture the full effect of the surface eddies. Refining the mesh could thus be a good option in order to have a more precise simulation but we need to focus about the total number of elements in order to avoid needing too much resources.
Finally, we've shown that the parametrization of our model and especially the turbulent closure model have a direct effect on the results we get. More studies and simulation might thus be needed in order to find the perfect turbulent closure model that will help us match the collected data.

5.4 Conclusion

This thesis provided a deep explanation of the development of a simulation based on the hydrodynamic model SLIM. It also provided the different results obtained with that methodology. It had as objective to build a complete model that would give us realistic results. These results are a first step towards the estimation of the environmental impact of deep-sea mining. Unfortunatelythe current simulation models did not yield satisfactory results and could therefore not be validated. We gave some possible reasons that could explain the failure of the simulations and that can be further examined.
In order to develop this study further more and to arrive at a validation of a simulation it will be important to collect more information about the deep-sea. Those could help develop the global understanding of deep-sea currents even further. It will also help us to be more critical towards the different data collected and to target the gaps of our simulation in order to correct them. To develop that deepening quickly, a greater sharing of the data between the different companies involved into the deep-sea mining is needed. But that cooperation contradicts the actual industrial mentality and would thus probably not happen for the moment.

Appendix A

The approximations

A.1 The Boussinesq approximation

In this section we will develop the Boussinesq approximation The Boussinesq approximation is stated as follow:

$$\frac{\Delta\rho}{\rho\cdot} << 1 \tag{A.1}$$

With $\Delta\rho$ being the difference of density in our environment and $\rho\cdot$ being the reference value of the water density ($1027[kg/m^3]$ for SLIM). This approximation is thus validate if the variation of density is small compared to its mean value. In our zone, water is the major constituent, the density variations will thus be small. Indeed, assuming that our zone can be represented by the point 14,6N and 125.6W (point in the zone B4), we can calculate the variation of density between the bottom of the ocean and the top of it. The density is calculated thanks to the salinity and the temperature on the following site: `http://fermi.jhuapl.edu/denscalc.html`). We arrive at a maximum density on at 4500m deep, with a temperature of 1.4°C and a salinity of 34.7 psu. The maximum density found for those values is of $1050[kg/m^3]$. On the top of the ocean, we've got a maximum temperature of 28°C and a minimum salinity of 34 psu, which gives a density of $1021[kg/m^3]$. The difference of density being quite small compared to the reference density value, the Boussinesq approximation is thus validated.

$$\begin{aligned} \frac{\Delta\rho}{\rho\cdot} &<< 1 \\ \frac{\Delta\rho}{\rho\cdot} \approx \frac{30}{1027} &<< 1 \end{aligned} \tag{A.2}$$

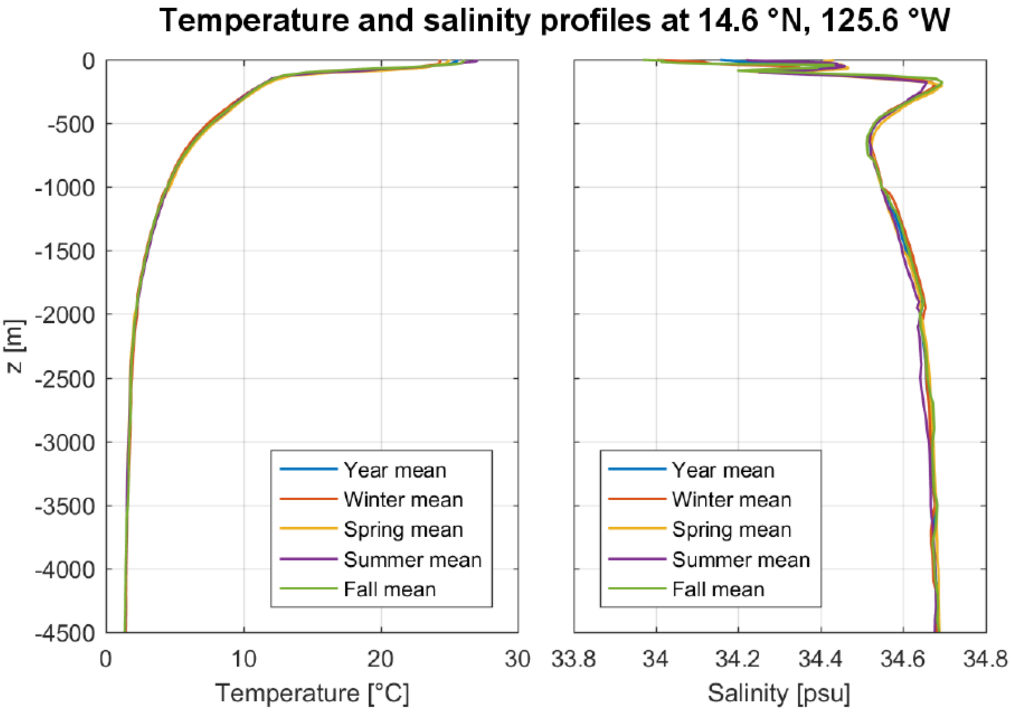

Figure A.1: Mean temperature[29] and salinity[28] profile used to compute the density.

Appendix B

The turbulent closure models

B.1 GOTM

GOTM (General Ocean Turbulence Model)is a library who proposes a generic turbulent closure model. That model can then be adapted to obtain different types of turbulent closure models. To do so you just have to change the parameters. The generic model used by GOTM is (Umlauf Burchard, J. Mar. Res., 2003 [30]) closure model and SLIM3D is coupled to the $\kappa - \epsilon$ turbulence closure model[31].

B.2 Pacanowski & Philander

When changing to the Pacanowski Philander's turbulent closure model change the formulation of the vertical viscosity ν and of the vertical diffusivity κ.

For the vertical viscosity, the formula is the following:

$$\nu = \nu_B + \frac{\nu_0}{(1 + \alpha Ri)^n} \tag{B.1}$$

And for the vertical diffusivity, we have:

$$\kappa = \kappa_B + \frac{\nu}{(1 + \alpha Ri)} \tag{B.2}$$

where

- $Ri = \frac{N^2}{M^2}$, is the Richardson number.
- $N^2 = max(0, -\frac{g}{\rho_0}\frac{d\rho}{dz}))$, is the Brunt-Väisälä frequency.
- $M^2 = norm(\frac{du}{dz})$, is the square of the shear frequency.

- ν_B, is the background viscosity (the default value is 1e-5).
- ν_0, is the maximal viscosity (the default value is 1e-2).
- α, is a factor for Ri (the default value is 10).
- n, is a exponent factor for the denominator (the default value is 2).
- κ_B, is the background diffusivity (the default value is 1e-5).

Appendix C

Results

C.1 Vertical extrusion of the mesh

N	z [m]	Δ z [m]	N	z [m]	Δ z [m]
1	0	4	27	-1500	500
2	-4	4	28	-2000	500
3	-8	2	29	-2500	500
4	-10	5	30	-3000	500
5	-15	5	31	-3500	500
6	-20	5	32	-4000	200
7	-25	10	33	-4200	100
8	-35	10	34	-4300	50
9	-45	15	35	-4350	30
10	-60	20	36	-4380	20
11	-80	20	37	-4400	20
12	-100	25	38	-4420	20
13	-125	25	39	-4440	20
14	-150	50	40	-4460	20
15	-200	50	41	-4480	20
16	-250	50	42	-4500	20
17	-300	50	43	-4520	20
18	-350	50	44	-4540	20
19	-400	100	45	-4560	20
20	-500	100	46	-4580	20
21	-600	100	47	-4600	50
22	-700	100	48	-4650	50
23	-800	100	49	-4700	100
24	-900	100	50	-4800	400
25	-1000	200	51	-5200	166
26	-1200	300	52	-5366	0

Figure C.1: Vertical mesh spacing for the maximum depth (5366m). In red are the σ-layers and in black the z-layers. N is the index of the layer, z is the depth and Δz is the distance from the next layer.

Bibliography

[1] DEME: Deep sea mining can support the circular economy
http://www2.deme-group.com/news/deep-sea-mining-can-support-circular-economy

[2] Greenspec: Copper production & environmental impact
https://www.greenspec.co.uk/building-design/copper-production-environmental\-impact/

[3] The Guardian, Damian Carrington (2017): Is deep sea mining vital for a greener future 3 even if it destroys ecosystems?
https://www.theguardian.com/environment/2017/jun/04/is-deep-sea-mining-vital-for-greener-future-even-if-it-means-destroying-preciou

[4] Laurent White, Eric Deleersnijder, Vincent Legat, A three-dimensional unstructured mesh finite element shallow-water model, with application to the flows around an island and in a wind-driven, elongated basin, Ocean Modelling, Volume 22, Issues 1–2, 2008, Pages 26-47, ISSN 1463-5003, https://doi.org/10.1016/j.ocemod.2008.01.001. http://www.sciencedirect.com/science/article/pii/S1463500308000140

[5] European Commission : Cobalt: supply and demand balances in the transition to electric mobility
https://ec.europa.eu/jrc/sites/jrcsh/files/cobalt_infographics_one-pager.pdf

[6] Amnesty: Is my phone powered by child labour?
https://www.amnesty.org/en/latest/campaigns/2016/06/drc-cobalt-child-labour/

[7] Wikipedia: Rare earths trade dispute
https://en.wikipedia.org/wiki/Rare_earths_trade_dispute#:~:text=Dispute%20arose%20when%20the%20Chinese,move%20was%20protectionism%20in%20disguise

[8] European Commission: Critical raw materialsrix
https://ec.europa.eu/growth/sectors/raw-materials/specific-interest/critical_en

[9] International Seabed Authority: Clarion Clipperton Zone Exploration Area
https://www.isa.org.jm/map/clarion-clipperton-fracture-zone

[10] ISA : Protection of the Marine Environment
https://www.isa.org.jm/our-work/protection-marine-environment

[11] Global Sea Mineral Ressources: Environmental Impact Statement
Avalaible: https://economie.fgov.be/en/themes/enterprises/deep-sea-mining/workshops-and-public/environmental-impact-statement

[12] International Union for Conservation of Nature : Deep-sea mining https://www.iucn.org/resources/issues-briefs/deep-sea-mining

[13] Thomas Peacock: TEDxMIT: Mining the deep-sea https://www.ted.com/talks/tom_peacock_mining_the_deep_sea

[14] Barbie Bischof, Elizabeth Rowe, Arthur J. Mariano, Edward H. Ryan: The North Equatorial Current
https://oceancurrents.rsmas.miami.edu/atlantic/north-equatorial.html

[15] Cooper, Alan; Day, K. (2015): TELEMAC-3D and Hydrostatic Inconsistency.
https://henry.baw.de/bitstream/20.500.11970/104312/1/11_Cooper_2015.pdf

[16] Jackett, D. R., McDougall, T. J., Feistel, R., Wright, D. G., and Griffies, S. M. (2006). Algorithms for Density, Potential Temperature, Conservative Temperature, and the Freezing Temperature of Seawater. Journal of Atmospheric and Oceanic Technology, 23(12):1709-1728.

[17] Burchard, H., Bolding, K., Villarreal, M.R., 1999. GOTM, a general ocean turbulencemodel. Theory, implementation and test cases. Technical Report EUR 18745,European Commission.

[18] Chassignet, E. P., Hurlburt, H. E., Smedstad, O. M., Halliwell, G. R., Hogan, P. J., Wallcraft, A. J., Baraille, R., and Bleck, R. (2007). The HYCOM (HYbrid Coordinate Ocean Model) data assimilative system. Journal of Marine Systems, 65(14):60-83.

[19] Egbert, G. D. and Erofeeva, S. Y. (2002). Efficient inverse modeling of barotropic ocean tides. Journal of Atmospheric and Oceanic Technology, 19(2):183-204.

[20] Kessler W.S. (2006). The circulation of the eastern tropical Pacific: A review. Progress in Oceanography, 69(2–4), 181–217, doi: 10.1016/j.pocean.2006.03.009.

[21] IMDC : WP2: Synthetis report site characterisation (Delivery D2.0)

[22] Rebesco M., Hernández-Molina F.J., Van Rooij D. Wåhlin A. (2014). Contourites and associated sediments controlled by deep-water circulation processes: State-of-the-art and future considerations. Marine Geology, 352, 111–154, doi: 10.1016/j.margeo.2014.03.011.

[23] Towards a physical model of Antarctic sea ice microstructure including biogeochemical processes using the extended Theory of Porous Media - Scientific Figure on ResearchGate.
https://www.researchgate.net/figure/Temperature-salinity-graph-showing-lines-of-fig3_335607252

[24] Cushman-Roisin B. Beckers J.-M. (2011). Introduction to geophysical fluid dynamics: physical and numerical aspects. Academic Press.

[25] Aleynik, D., Inall, M.E., Dale, A. et al. Impact of remotely generated eddies on plume dispersion at abyssal mining sites in the Pacific. Sci Rep 7, 16959 (2017). https://doi.org/10.1038/s41598-017-16912-2

[26] General Bathymetric Chart of the Oceans (2019)
https://download.gebco.net/

[27] Eric Deleersnijder (2018): Modelling transport processes in geophysical and environmental flows Downloaded from: https://moodleucl.uclouvain.be

[28] Zweng M.M., Reagan J.R., Antonov J., Locarnini R.A., Mishonov A.V., Boyer T.P., Garcia H.E., Baranova O.K., Johnson D.R., Seidov D. Biddle M.M. (2013). World Ocean Atlas 2013, Vol. 2, Salinity.

[29] Locarnini R., Mishonov A.V., Antonov J., Boyer T., Garcia H., Baranova O.K., Zweng M.M., Paver C.R., Reagan J.R., Johnson D., Hamilton M. Seidov D. (2013). World Ocean Atlas 2013, Volume 1: Temperature.

[30] Umlauf, L., Burchard, H., 2003. A generic length-scale equation for geophysical turbulence models. Journal of Marine Research 235–265 (31).

[31] Kärnä, T., Legat, V., Deleersnijder, E., and Burchard, H. (2012). Coupling of a discontinuous Galerkin finite element marine model with a finite difference turbulence closure model. Ocean Modelling, 47:55-64.

UNIVERSITÉ CATHOLIQUE DE LOUVAIN
École polytechnique de Louvain
Rue Archimède, 1 bte L6.11.01, 1348 Louvain-la-Neuve, Belgique | **www.uclouvain.be/epl**